Practical Wind Turbine Selection: A Multicriterion Decision Analysis for Sustainable Energy Infrastructure

Mohammad Naseer Zakir[1]; Abdul Rahman Abasin[2]; Ahmad Shah Irshad[3]; Said Elias[4]; Atsushi Yona[5]; and Tomonobu Senjyu[6]

Abstract: In the pursuit of a sustainable energy future, this study employs multicriteria decision analysis (MCDA) to present a concise and comprehensive strategy for onshore wind project cost analysis, addressing the critical consideration of structural stability under survival wind loads. Navigating the challenges of the contemporary industrial economy, including escalating energy costs, supply uncertainties, and environmental concerns, the research explores turbine selection based on power factor considerations, economic evaluations, and a meticulous wind resource assessment using the robust Weibull distribution. Recognizing the economic advantages of proximity between power generation sources and load centers, the study introduces the groundbreaking E-115 model, a cost-effective wind turbine. Evaluation metrics, including the levelized cost of energy (LCOE), simple payback period (SPP), net present value (NPV) per kW, benefit-to-cost ratio (BCR), internal rate of return (IRR), and cost of turbine per kW, underscore the robust viability and economic advantages of the E-115 model. Beyond economic considerations, the research emphasizes structural stability for resilience under survival wind loads and highlights the potential of wind turbines to reduce greenhouse gas emissions by 97.26% compared to coal power plants. Positioned as a central force in steering nations toward responsible and eco-conscious development, wind energy emerges as a transformative and imperative component of the sustainable energy landscape. The study's implications extend beyond numerical revelations, providing a foundation for future research and policy decisions, shaping the discourse around renewable energy, and offering insights that transcend mere statistics to chart a course toward a greener, more resilient future. **DOI: 10.1061/PPSCFX.SCENG-1508.**

Author keywords: Sustainable energy; Structural stability; Wind turbine selection; Economic viability; Renewable energy.

Introduction

The imperative of energy provision stands as a linchpin for human development and societal progress. Fueling nearly every facet of modern life, from basic necessities like cooking and lighting to complex systems such as healthcare, education, and industrial production, energy infrastructure is at the core of civilization's evolution. However, the challenges posed by escalating energy prices, supply uncertainties, environmental apprehensions, and nuclear energy complexities have spurred a global quest for alternatives to conventional fossil fuel reserves. In this transformative landscape, renewable energy technologies have witnessed unprecedented advancements, with wind energy emerging as the vanguard, boasting a remarkable 27% growth in the last five years (Abbes and Belhadj 2012; Al-Dousari et al. 2019; Irshad 2023; Ibrahim and Albani 2016).

The trajectory of a nation's modernity is now intrinsically tied to its per capita energy consumption. Energy is not merely a commodity; it is the catalyst for economic development and a determinant of quality of life. The current abundance of energy has catalyzed increased productivity, shortened workdays, improved nutrition, and enhanced transportation. The very origin of this energy abundance lies in the sun, the primary source sustaining life on Earth. Even wind and tidal energy, products of solar-induced climate and weather patterns, owe their existence to the sun's influence. Photosynthetic technologies further contribute to this abundance, giving rise to oil, natural gas, coal, and wood through intricate chemical processes involving the transformation of decaying plants over extensive periods (Kalogirou 2014; González et al. 2011; Shah et al. 2023; Noori et al. 2022; Irshad and Noori 2022).

Recognizing that energy-related carbon dioxide (CO_2) emissions account for a substantial two-thirds of all greenhouse gases (GHG), transitioning to low-carbon alternatives becomes imperative (Gielen et al. 2019). Technological strides in renewable energy, particularly in solar photovoltaic (PV) and wind power, have driven down prices and enhanced competitiveness, resulting in record additions of installed renewable energy generating capacity.

The realm of alternative energy, free from fossil fuel dependency, emerges as an environmental and accessible solution. Hydropower, wind, solar, geothermal, and biofuels represent renewable alternatives with minimal environmental impact. Globally, in 2015, renewable energy constituted 11% of the total energy produced, with wind contributing a significant 19%. Wind power, expanding

[1]Dept. of Energy Engineering, Engineering Faculty, Kandahar Univ., Kandahar 3801, Afghanistan (corresponding author). Email: nasirzakir8@gmail.com

[2]Dept. of Energy Engineering, Engineering Faculty, Kandahar Univ., Kandahar 3801, Afghanistan. ORCID: https://orcid.org/0009-0000-9692-2656

[3]Dept. of Energy Engineering, Engineering Faculty, Kandahar Univ., Kandahar 3801, Afghanistan; Dept. of Electrical and Electronics Engineering, Faculty of Engineering, Univ. of the Ryukyus, Okinawa 903-0213, Japan.

[4]Marie Skłodowska-Curie Actions (MSCA) Postdoctoral Fellow, Institute for Risk and Reliability, Leibniz Univ. Hannover, Callinstr, Hannover 3430167, Germany. ORCID: https://orcid.org/0000-0002-8231-9765. Email: elias.rahimi@irz.uni-hannover.de

[5]Professor, Dept. of Electrical and Electronics Engineering, Faculty of Engineering, Univ. of the Ryukyus, Okinawa 903-0213, Japan.

[6]Professor, Dept. of Electrical and Electronics Engineering, Faculty of Engineering, Univ. of the Ryukyus, Okinawa 903-0213, Japan.

Note. This manuscript was submitted on November 21, 2023; approved on January 23, 2024; published online on April 18, 2024. Discussion period open until September 18, 2024; separate discussions must be submitted for individual papers. This paper is part of the ***Practice Periodical on Structural Design and Construction***, © ASCE, ISSN 1084-0680.

Table 1. Imported electricity tariffs of 2018 year Da Afghanistan Brishna Sharkat

Exporter country	2018 (January to June) in USD	2018 (July to December) in USD
Uzbekistan	0.0765	0.0500
Tajikistan (220 kV transmission line)	0.0418	0.0418
Tajikistan (Pamir Badakhshan)	0.0350	0.0350
Tajikistan (110 kV transmission line)	0.0300	0.0300
Turkmenistan	0.0400	0.0400

at a remarkable 34% annual pace in 2011, stood as the second-fastest-growing renewable energy source (Li et al. 2015). In an era of heightened environmental consciousness, a single 1 MW wind turbine (WT) annually offsets 27.22 kg of mercury, three tons of nitrogen oxides, 1,500 tons of carbon dioxide, and 6.5 tons of sulfur dioxide. Remarkably, compared to coal plants (11 times) and nuclear reactors (16 times), wind farms yield between 17 and 39 times more energy than they consume (Siddique and Wazir 2016). Globally, researchers are exploring multiterminal DC grids as a solution to connect renewable energy sources, distributed generators, and HVDC transmission lines to the grid (Ludin et al. 2023).

Afghanistan, at the cusp of energy evolution, boasts an installed generating capacity of 568 megawatts (MW) as of December 31, 2018. This capacity comprises a nuanced mix: 53% (300 MW) from the majestic flow of hydropower, 35% (200 MW) harnessed from thermal plants fueled by diesel and heavy fuel oil, and 11% (65 MW) from the relentless embrace of solar generators (Rostami et al. 2017). The majority of this dynamic energy ensemble is orchestrated by a select few hydroelectric units strategically dispersed across the nation. In the bustling hub of Kabul, thermal power plants stand sentinel as reliable backup power, while miniature generators illuminate provinces without access to the main grid.

Afghanistan's energy narrative pivots on a critical axis, the importation of approximately 80% of its electricity. This import-driven reality renders the import price a linchpin in shaping the nation's electricity tariff, a fee delicately tailored for various customer categories, each intricately woven with the unique origin of its electrical genesis. Table 1 meticulously articulates the tariffs, dissecting the cost structure for imported electricity from diverse sources (IRENA 2018).

Yet, the energy tableau shifts dramatically in Kandahar province, where demand surges against the backdrop of limited existing resources. Remote districts, nestled in the rugged expanse, find themselves yearning for the glow of electricity, a luxury denied by the tyranny of high transmission costs. Here, solar and wind emerge as not mere alternatives but as the veritable lifeblood, abundantly available and waiting to be harnessed. The quest to satiate the energy thirst of these remote districts assumes an imperative hue, the power generation source must nestle close to the load center, strategically placed to perform with demand while sidestepping the burdens of exorbitant transmission costs.

As Afghanistan grapples with the intricate lack of supply and demand, this energy landscape underscores the pivotal role played by import prices, shaping tariffs that ripple across the socioeconomic fabric. In Kandahar, the synergy of solar and wind beckons as a beacon, not just meeting but transforming the energy needs of remote districts. The quest for proximity between power generation and load centers signals a revolutionary approach, untethering remote regions from the shackles of transmission costs and propelling them into the era of accessible and sustainable energy.

Over the last two dynamic decades, a symphony of ingenuity has echoed across the wind energy landscape, resonating in various models and methodologies aimed at optimizing the selection of wind turbines. This visionary pursuit, guided by economic analysis and mathematical modeling, has not only shaped the trajectory of onshore and offshore wind energy but has also sparked the evolution of cutting-edge commercial software packages dedicated to this cause.

In the realm of audacious endeavors, the prospective NEOM city in Saudi Arabia stands as a testament to the transformative potential of wind energy. In a critical assessment encapsulated by Alfawzan et al. (2020), the wind energy potential of this visionary city is meticulously unraveled. The defining criterion for turbine selection? A delicate performance between the highest capacity factor and the lowest levelized cost of energy (LCOE). This strategic marriage of performance and efficiency charts a course toward sustainable energy excellence.

Venturing into the heart of the central area of Thailand, Quan and Leephakpreeda (2015) takes us on a journey of exploration through compelling case studies. Here, wind analysis intertwines with economic scrutiny, creating a harmonious synergy that unveils the true possibilities of electrical energy generation from commercial wind turbines. An innovative directional limitation mechanism, as espoused by Sun et al. (2020), emerges as a beacon of efficiency, particularly where prevailing wind directions carve a clear path for optimization.

Diving into uncharted territories, Rakhshani et al. (2020) pioneers a groundbreaking method for designing wind-diesel-battery systems. This ingenious approach positions wind turbine technology as the linchpin, allowing it to wield unparalleled influence among the myriad options available. The orchestration of wind energy potential assessment and turbine selection, as envisioned by Abbes and Belhadj (2012), unveils a meticulous microsifting process using Windstation and 3DEM software, transcending traditional norms.

Rooted in statistical prowess, Wang et al. (2018) builds a selection strategy foundation on the root-mean-square error. This optimal statistical model, bolstered by simulated calculations grounded in the Weibull distribution, charts a course toward precision in the assessment and analysis of wind energy. In a realm where offshore wind farms beckon, Feng and Shen (2017) delves into the design intricacies of non-uniform configurations, ushering in a new era of variety in wind turbine types and hub-heights.

A symphony of methodologies, including the TSMI-TCI approach Ibrahim and Albani (2016) and Muche et al.'s (2016) economic idealism, further enriches our understanding. The pursuit of excellence reaches new heights in a case study of wind turbine selection at Brfell, Iceland, where evolutionary computing methodologies and an astute cost model converge (Perkin et al. 2015). The revelation of a top-performing hypothetical wind turbine design, outshining the current Enercon E-44 WTs, signifies not just progress but a leap toward economic efficiency, reducing the LCOE by 10.4%.

In the diverse landscapes of Central Turkey, Gokcek and Serdar (2009) scrutinizes the cost of wind energy through the lens of the LCOE approach, unraveling considerations of yearly mean speed and the escalation ratio of operating and maintenance costs. Departing from the technically feasible, Muche et al.'s method (2016) propels us into the realm of economic idealism, where horizontal axis wind turbine configurations are meticulously tailored to maximize net present value. The intricate performance between size parameters and economic parameters, accentuated by the impact of yearly mean speed and the escalation ratio of operating and maintenance costs on LCOE, reveals a compass pointing toward economically optimal wind energy solutions.

In this resounding crescendo of innovative methodologies, the wind energy landscape not only unfolds but evolves into a symposium of possibilities, promising not just efficiency but a paradigm shift in the very fabric of our energy future.

As we traverse the windswept landscapes of wind energy innovation, our narrative converges on the rugged expanse of Afghanistan. A nation endowed with substantial wind energy potential; Afghanistan's western frontier witnesses the performance of strong winds for over four months each year. Bounded by South Asian neighbors with China, Pakistan, Iran, Turkmenistan, Uzbekistan, Tajikistan, and Afghanistan emerges as a nexus, a frontier in the realm of renewable energy possibilities.

Consulting the authoritative National Renewable Energy Laboratory wind map, we find a canvas of promise spread across a 31,611 km^2 region, where winds ascend above class 4, characterized by speeds exceeding 6.8 m/s and an energetic 400 W/m^2 (Noori et al. 2019). In this wind-kissed expanse, envisioning the deployment of 5MW turbines per km^2 unveils an awe-inspiring 158.1 GW capacity for wind power installations (Elliott 2011). The intricacies of this wind power potential are meticulously mapped, revealing a landscape ripe for utility-scale wind turbines in class three locations (wind speeds over 6.1 m/s), covering an expansive 98,851 km^2 (Anwarzai and Nagasaka 2014). Wind power potential map and its categorization were provided by Anwarzai and Nagasaka (2014). This wind energy extends beyond theoretical calculations, as we gaze upon the wind power potential map, a visual testament to the untapped energy woven into Afghanistan's tapestry. The entire accessible area above class three beckons, a vast expanse of opportunity awaiting harnessing and transformation.

Delving deeper into the numerical realm, the yearly wind energy site potential, a staggering 0.34×10^9 GWh, unfurls before us. Yet, cognizant of the pragmatic complexities, we acknowledge that not all this potential can be seamlessly realized. The need for further investigation and dedicated research becomes apparent, paving the way for the practical implementation of this latent energy potential.

Amidst this canvas of promise, Afghanistan stands at the threshold of a new energy era. The nation's renewable energy agency has sown the seeds of change with 22 wind energy projects, six of which have already come to fruition, boasting a cumulative capacity of 230 kW (Anwarzai and Nagasaka 2014). While large-scale, grid-connected wind power generation plants are yet to grace the Afghan terrain, these nascent projects exemplify the nation's fervent commitment to embracing the winds of change.

In this symphony of wind energy potential, Afghanistan emerges not merely as a geographic entity but as a crucible of possibilities, where the winds whisper not just of energy but of transformation and sustainable progress. As our narrative unfolds, Afghanistan's journey into the realm of renewable energy becomes a beacon, illuminating a path toward harnessing the untapped vigor of the wind, and, in doing so, propelling the nation into a future powered by sustainable and forward-thinking energy solutions.

Building upon the windswept foundation of global wind energy advancements and Afghanistan's untapped potential, our present study unfurls with a bold aim to bridge the existing gap in literature by crafting a groundbreaking methodology for onshore wind farm projects. In a symphony of innovation, we traverse the diverse terrain of wind resource assessment, turbine selection, and cost analysis, collectively creating a paradigm shift in Afghanistan's pursuit of sustainable and electrified futures.

The economic intricacies of wind energy in Afghanistan, largely unexplored till now, become the focal point of our study. As pioneers on this uncharted frontier, our contributions resonate through the very fabric of the nation's energy landscape. Our objectives extend beyond conventional studies, aiming to:

- *Provide a Comprehensive Methodology*: We lay the groundwork for a holistic methodology, unraveling the intricate performance between wind energy resources, turbine selection, and cost analysis for onshore wind projects in Afghanistan. This is not merely a study; it is a blueprint for a new era in sustainable energy planning.
- *Offer a Simple Yet Accurate Approach*: In the complexity of wind turbine selection, we present a beacon of simplicity. Our study offers a streamlined yet precise method for choosing the most suitable and cost-effective wind turbine configurations, tailored specifically for the Afghan landscape.
- *Analyze Hourly Data with Precision*: We delve into the minutiae of wind energy potential, eschewing tradition for precision. Analyzing hourly data over four years, we employ the robust Weibull distribution, elevating our assessments beyond the limitations of conventional methods.
- *Estimate Comprehensive Turbine Costs*: Our study pioneers in cost modeling, scrutinizing not just the superficial expenses but the totality of each turbine's cost. Mechanical, electrical, control, auxiliary systems, and infrastructure all are factored in, offering a panoramic view of economic viability.
- *Apply Varied Metrics for Optimization*: Metrics such as NPV, IRR, LCOE, BCR, and SPP are not just acronyms; they are the compass guiding us to the optimal turbine for a selected site. Our approach transcends singular metrics, offering a nuanced understanding of economic efficiency.
- *Conduct a Green Economic Symphony*: Beyond numbers, our study orchestrates a comprehensive economic analysis of wind farm design, harmonizing economic feasibility with environmental stewardship. Greenhouse gas emissions reduction becomes a keynote in our symphony.
- *Initiate Afghanistan's First-Ever Wind Energy Economic Analysis*: In this pioneering expedition, our study stands as the vanguard of Afghanistan's maiden economic analysis of wind energy. It is not just a first; it is a transformative moment, a cornerstone for future renewable energy endeavors.
- *Empower Sustainable Development*: Beyond academic pursuits, our study resonates with the heartbeat of sustainable development. It becomes a catalyst for change, an instrument in the hands of a nation striving for a greener, more electrified tomorrow.

As the winds of progress intertwine with our aspirations, this study becomes not just a scholarly endeavor but a herald of change, shaping the narrative of renewable energy in Afghanistan and setting the stage for a future powered by the boundless potential of wind.

Structural Safety of Wind Turbines

The first important step to be confident that the selected wind turbines contain required structural safety to stand during the windy season. Fig. 1 illustrates the pertinent structural information concerning the chosen wind turbines. Based on structural safety consideration, it is seen that the cutoff wind velocity for the selected wind turbines is 25 m/s. Although, based on the design principals they have been designed for at least up to a wind velocity of 50 m/s, which is called survival wind velocity (see Fig. 1). Fig. 1 provides a comprehensive view of various structural configurations of wind turbines, each meticulously designed to withstand specific survival wind speeds. The survival wind speed, representing the maximum wind intensity a turbine is engineered to endure, is a critical factor influencing its structural integrity and overall resilience. In part (a) of the figure, the horizontal axis remains common, representing different wind turbine models. The vertical axis, however, encapsulates the variation of rotor diameter and hub height for

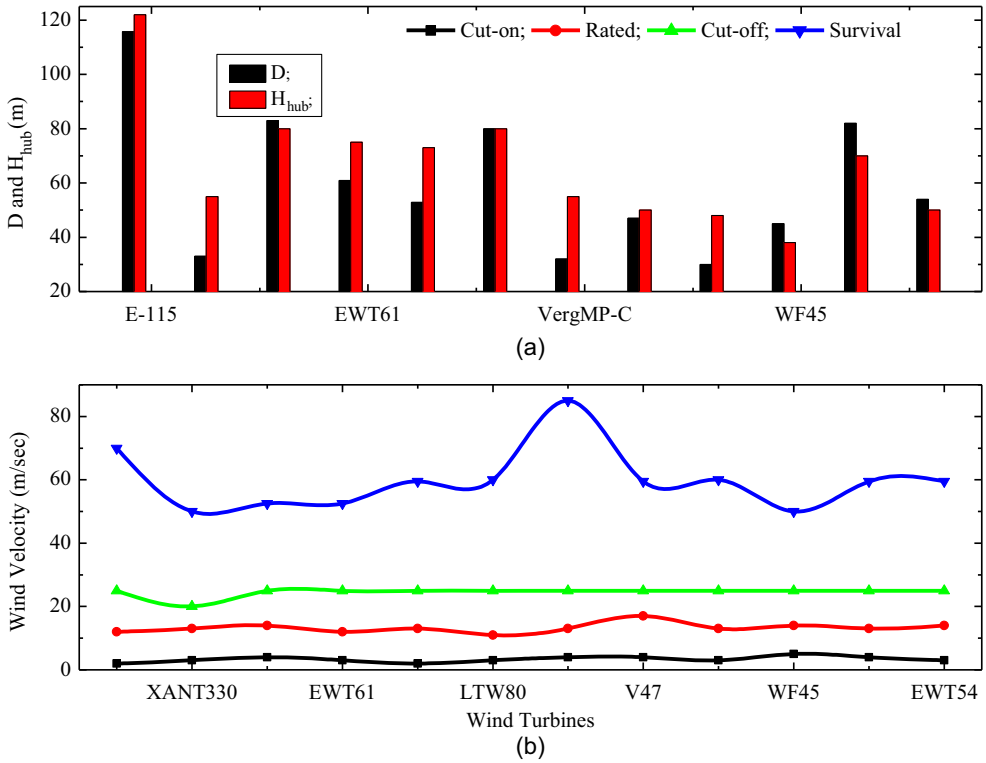

Fig. 1. Structural configurations of wind turbines with their survival limits: (a) variation in rotor diameter and hub height across different wind turbine models; and (b) operational and survival characteristics of wind turbine models.

each turbine. This variation illustrates the adaptability of different designs to optimize performance under diverse wind conditions. In part (b) of Fig. 1, the common horizontal axis depicts the specified wind turbine models, while the vertical axis introduces a set of wind velocity curves. Four distinct curves unfold the operational characteristics: the *cut-on* curve signifies the minimum wind speed required for turbine initiation, the *trade* curve represents the optimal wind velocity for efficient operation, and the *cut-off* curve marks the wind speed at which turbines cease operation. Additionally, a crucial *survival* curve outlines the wind turbine's maximum capacity, showcasing the highest wind speed each model can endure under extreme wind loading conditions. This holistic representation of wind velocities provides a comprehensive insight into the operational thresholds and survival limits of the depicted wind turbine designs, crucial for understanding their performance characteristics in varying environmental conditions.

In the labeled configurations, the first design (labeled E-115) exhibits a slender tower and expansive blades, demonstrating optimization for regions with relatively moderate wind conditions. The survival limit, illustrated by the shaded region in Fig. 1, indicates the maximum wind speed at which this design remains structurally sound, ensuring longevity and safety. Moving to the other configuration (labeled VergMP-C), a more robust and compact design is evident. This configuration is specifically tailored for regions where wind speeds can reach higher extremes. The extended survival limit reflects the incorporation of enhanced structural elements to endure the challenges posed by more demanding environmental conditions.

The diversity in structural configurations depicted in Fig. 1 emphasizes the nuanced relationship between form and function in wind turbine design. The survival limits serve as crucial benchmarks for engineers and developers, guiding the optimization of each turbine for performance and ensuring it is constructed to withstand the unique challenges of its operating environment. This figure serves as a visual representation of the intricate balance between structural considerations and the dynamic forces imposed by wind conditions. It reinforces the importance of tailoring wind turbine designs to specific survival wind speeds, thereby enhancing their efficiency, safety, and longevity across diverse geographical contexts. It should be noted that the soil effect must not be overlooked when considering the structural safety of wind turbines (Gaur et al. 2020; Elias 2024).

Wind Energy and Methodology

In charting a pioneering course for onshore wind farm projects in Afghanistan, our methodology unfolds through a meticulous process encompassing site selection, international electro-technical commission (IEC) classes determination for wind turbines, and a nuanced exploration of wind speed distribution and characteristics. Each facet of our approach is intricately designed to navigate the complex terrain of Afghanistan's unique wind energy landscape, laying the foundation for a comprehensive evaluation that transcends traditional boundaries.

Site Selection: Pioneering the Windswept Frontier

The step-by-step methodology diagram of the research is illustrated in Fig. 2, offering a visual roadmap for the groundbreaking journey undertaken in this study. In the intricate tapestry of Afghanistan's diverse landscapes, our site selection process emerges as a strategic masterpiece. Amidst the nation's 8 divisions, 34 provinces, and 364 districts, Kandahar, a southern province, takes center stage with its 17 districts. Within the heart of this province lies Reg District, a sun-soaked expanse with just a few villages scattered across its desert terrain, home to 7,752 resilient individuals as of 2020. Situated

Pract. Period. Struct. Des. Constr., 2024, 29(3): 04024028

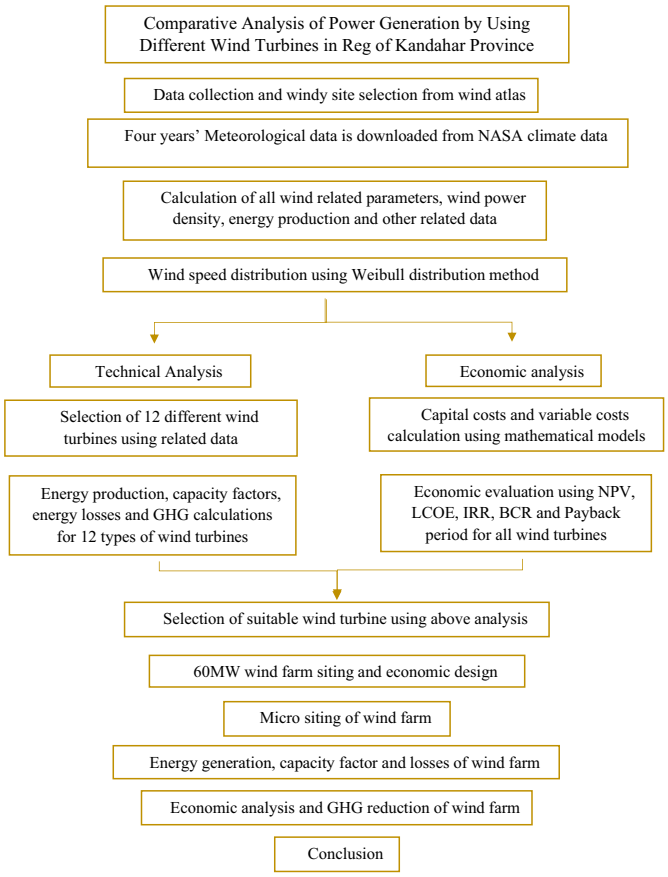

Fig. 2. Step-by-step methodology diagram of the research.

near the international border with Pakistan, this district's administrative hub paints a picture of isolation and arid beauty.

Our selected site, strategically positioned at the crossroads of Helmand to the west and Pakistan to the south, embodies the potential for a wind-powered revolution. The meticulous process of site selection unfolds through the lens of the global wind atlas (GWA) (Davis et al. 2023) and the intricate scrutiny afforded by Google Earth. The coordinates, a geographical ballet at 29.72443° latitude and 64.57695° longitude, movement on the canvas of Reg District, Kandahar province, Afghanistan, as depicted in Fig. 3.

This study does not just rely on geographic coordinates; it leverages the power of GWA, the National Aeronautics and Space Administration (NASA), prediction of worldwide energy resources (POWER), and Google Earth to identify a high-wind site—a strategic choice backed by meteorological data downloaded from NASA POWER. The selected site, spanning approximately 360 km^2, unfolds as a canvas for innovation, where the average wind speed and power density, meticulously outlined on the global map by GWA, converge with the topography viewed through the lens of Google Earth.

In this groundbreaking endeavor, the selected site is not just a geographical point; it is a beacon for the convergence of data, technology, and the relentless Afghan spirit. As the winds of change whisper through the desert expanse, this site becomes the canvas upon which the future of wind energy in Afghanistan is painted.

IEC Classes of Wind Turbines: Navigating the Wind's Symphony

In the realm of wind energy, the classification of wind turbines is not just a technicality; it is a strategic orchestration. Embracing the standards set by IEC61400, large Wind Turbines (WTs) wear the badge of IEC certification, a testament to their resilience in the face of diverse wind characteristics. As defined by IEC61400, the class of a wind turbine becomes a pivotal factor, delineating its compatibility with the unique wind dynamics of a specific site.

In this symphony of wind energy, each class resonates with a distinct purpose. Class I WTs stand as fortresses, engineered to brave the harshest conditions nature can unleash. As the wind's intensity subsides, Class III WTs gracefully step in, tailored for locations with more modest wind resources. Meanwhile, Class II WTs, with their expanded sweep area and elongated blades, take the stage in regions boasting medium wind resources. This strategic variation allows Class II and III WTs to not only endure but thrive, capturing wind energy even in the gentlest whispers of a breeze (Earnest and Rachel 2019). Beyond the classification, the IEC's metrics delve into the very essence of the wind's character. Turbulence, a term echoing the intensity variation of wind speed around a mean, becomes a critical consideration. It is measured as the simple ratio of wind speed standard deviation (SD) to mean wind speed. Yet, the IEC's discernment does not stop here; it extends to power performance, noise levels, and the intricate of electrical properties. In this groundbreaking exploration, the classification of wind turbines is not a mere technicality; it is a harmonious interplay

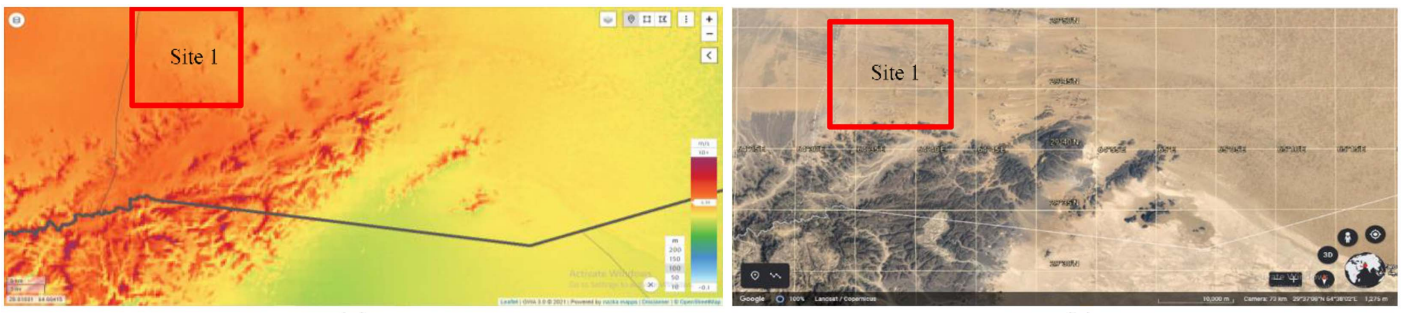

Fig. 3. Site images: (a) global wind atlas (GWA) site image [Reprinted under Creative Commons-BY-4.0 license (https://creativecommons.org/licenses/by/4.0/); image obtained from the Global Wind Atlas version 3.3, a free, web-based application developed, owned and operated by the Technical University of Denmark (DTU). The Global Wind Atlas version 3.3 is released in partnership with the World Bank Group, utilizing data provided by Vortex, using funding provided by the Energy Sector Management Assistance Program (ESMAP). For additional information: https://globalwindatlas.info]; and (b) Google Earth (GE) site image (map data © 2023 Google).

Pract. Period. Struct. Des. Constr., 2024, 29(3): 04024028

between engineering precision and the ever-changing cadence of the wind. As we navigate the symphony of IEC classes, the very essence of wind energy unfolds a strategic plan where each turbine class becomes a note, contributing to the melody of Afghanistan's wind-powered future.

Wind Speed Distribution and Characteristics: Unveiling the Winds' Mathematical Choreography

In the enchanting realm of wind energy, decoding the intricate of wind speed is an artistry accomplished through statistical analysis. At the heart of this analysis lies the utilization of probability functions, each a poetic expression of the statistical distribution of wind speed across diverse wind regimes. In the tapestry of wind energy mathematics, probability distribution functions (PDFs) emerge as the brushstrokes, capturing the irregular variations in wind speed with mathematical precision. Among the myriad mathematical representations, the Weibull distribution stands as a luminary, its elegance defined by two parameters that gracefully model the whims of the wind. This distribution becomes not just a mathematical abstraction but a tool of profound significance, fitting seamlessly into the contours of wind histograms. As illuminated by the works of Afanasyeva et al. (2016), Mohammadi et al. (2014), and Katsigiannis et al. (2013), the Weibull distribution emerges as the symphony conductor orchestrating the harmonious interplay of wind speed characteristics.

In this groundbreaking exploration, wind energy potential is not just a numerical abstraction; it is an unveiling of the winds' mathematical choreography. As we delve into the elegance of probability functions and embrace the nuances of wind speed distribution, each parameter becomes a note in the symphony of Afghanistan's wind-powered destiny. This section is not just an analysis; it is an ode to the winds, a testament to the marriage of mathematics and nature in the pursuit of a sustainable energy future

$$f(v) = \left(\frac{k}{c}\right)\left(\frac{v}{c}\right)^{k-1} e^{-\left(\frac{v}{c}\right)^k} \tag{1}$$

The wind speed's dimension is the same as the scale parameter of Weibull distribution, c. The parameter for the non-dimensional shape is k. The dimensionless form and scale characteristics are therefore computed using Afanasyeva et al. (2016), Mohammadi et al. (2014), Bahrami et al. (2019), and Eltamaly (2013)

$$k = \left(\frac{\sigma}{V}\right)^{-1.086} \tag{2}$$

$$c = \frac{v_{\text{avg}}}{\Gamma(1+1/k)} \tag{3}$$

The upper incomplete gamma function, or $\Gamma(x)$, has the following definition:

$$\Gamma(n+1) = n! \tag{4}$$

The equation as follows is used to compute the standard deviation (Chadee and Clarke 2018):

$$\sigma = \sqrt{c^2\left[\Gamma\left(1+\frac{2}{k}\right) - [\Gamma(1+1/k)]^2\right]} \tag{5}$$

The available power in the wind as a whole divided by the power determined by cube of average wind speed is known as the energy pattern factor, or K_e and it is used in the aerodynamic design of wind turbines Eq. (6):

$$k_e = \frac{1}{Nv^{-3}}\sum_{i=1}^{N} v^3 = \frac{\overline{v^3}}{v^{-3}} = \frac{\Gamma(1+3/k)}{\Gamma(1+1/k)} \tag{6}$$

where 35,064 is the number of bytes in a year, or N.

Four years of hourly data are evaluated monthly and annually to determine the average wind speed Eq. (7) (Chadee and Clarke 2018)

$$\bar{v} = \frac{1}{n}\sum_{i=1}^{n} v_i \tag{7}$$

To get the wind speed with greater energy, apply the formula (Adaramola et al. 2015) as follows:

$$v_{me} = c\left(\frac{k+2}{2}\right)^{\frac{1}{k}} \tag{8}$$

The following equation can be used to determine the area's most likely wind speed. (Adaramola et al. 2015):

$$v_{mp} = c\left(1-\frac{1}{k}\right)^{\frac{1}{k}} \tag{9}$$

An essential statistical parameter for evaluating wind energy potential and production is the cumulative distribution function F(v), which denotes the probability or time fraction of wind speeds being less than or equal to a specific value. This function can be depicted as follows (Adaramola et al. 2015):

$$F(v) = 1 - \exp\left[-\left(\frac{v}{c}\right)^k\right] \tag{10}$$

The log law is used in Wortman's (1982) mixing length type analysis, despite the fact that there are other approaches to anticipate a logarithmic wind profile (Muche et al. 2016; González et al. 2011)

$$\frac{v(z)}{v(z_r)} = \frac{In(z/z_o)}{In(z_r/z_o)} \tag{11}$$

where z_o = length of surface roughness that describes the roughness of the terrain with regard to mean wind speed, and $v(z)$ and $v(z_r)$ are the reference wind speeds at respective heights.

A wind rose is a figure that displays the azimuthal and temporal distribution of wind speed and direction at a displayed anemometer. Turbulence intensity is the most fundamental indicator of turbulence. It is determined by the ratio of the standard deviation to the mean wind speed

$$TI = \frac{\sigma_v}{\bar{v}} \tag{12}$$

The level of turbulence present in wind energy generation and potential is impacted by various factors, such as the average wind speed, surface texture, atmospheric stability, and topographical characteristics. Typically, this metric is assessed for a duration of up to an hour, with the wind energy engineering standard mandating a 10-minute timeframe.

Air density can cause big difference in power generation because the wind power is direct proportional to air density and air density is directed proportional to air pressure and inversely with temperature. For air density calculation, a simple formula is used (Jung and Schindler 2019)

$$\rho = \frac{\bar{P}}{R_d\bar{T}} \tag{13}$$

where R_d is 287 J/kg °K; T is temperature in Kelvin; and $\bar{P}$ is average pressure.

Assessing the wind resource available at a specific site can be best achieved by determining the wind power density. This method effectively measures the amount of energy accessible at the location and can be converted into electricity by a wind turbine. The wind power density, also referred to as wind power per unit area, is commonly denoted as Mohammadi et al. (2014), Chadee and Clarke (2018), and Adarmola et al. (2015)

$$\frac{P_w}{A} = \frac{1}{2}\rho \int_0^\infty v^3 f(v) dv = \frac{1}{2}\rho c^3 \Gamma\left(1 + \frac{3}{k}\right) \tag{14}$$

where A = total swift areas of WTs; v = wind speed; and ρ = density of air. Based on the observed data, the wind power density may be stated as follows (Bahrami et al. 2019; Chadee and Clarke 2018):

$$\frac{P_o}{A} = \frac{1}{2}\rho \frac{1}{n}\sum_{i=1}^{n} v_i^3 \tag{15}$$

where n is the quantity of measurement intervals. You may calculate the wind energy density by

$$\frac{\bar{E}}{A} = \left(\frac{\bar{P}}{A}\right)(N(\Delta t) \tag{16}$$

The annual energy output may be computed using

$$E_W = \sum_{I=1}^{N} P_W[v_T(\Delta t)] \tag{17}$$

Examples of qualitative wind resource magnitude assessments include

$$\frac{\bar{P}}{A} \approx 100\frac{W}{m^2} - \text{poor}, \qquad \frac{\bar{p}}{A} < 400\frac{W}{m^2} - \text{good},$$
$$\frac{\bar{p}}{A} > 700\frac{W}{m^2} - \text{great} \tag{18}$$

A typical statistic for determining a wind turbine's appropriateness on particular proposed locations is the capacity factor, which is created by dividing the estimated annual energy production (AEP) by the calculated nominal AEP using the following equation (Katsigiannis et al. 2013; Mohammadi et al. 2014; Ahmad et al. 2022):

$$C = \frac{E_{\text{total}}}{P_{\max} \times T_{\text{period}}} \tag{19}$$

The formula for the typical wind turbine power $\overline{P_W}$ is (Abbes and Belhadj 2014)

$$\overline{P_W} = \int_0^\infty P_W(v) f(v) dv \tag{20}$$

$P_W(v)$ is known as power curve of WT.

Capital Costs: Unveiling the Financial Canvas of Wind Energy

In the grand tapestry of wind energy ventures, the financial brushstrokes define the initial crescendo, a symphony of capital-intensive investments that echo through the project's lifespan. At the forefront of this financial overture stands the wind turbine, an emblem of both power and cost. Following closely in its wake, the grid connection unfurls as the second-highest cost element, weaving together the intricate performance of power distribution. As revealed by the meticulous review conducted by Blanco (2009), the capital cost casts a formidable shadow, potentially commandeering up to 80% of the entire project's lifespan cost. The nuances of this financial composition further unfold across global landscapes. In the fertile grounds of Europe, the price per kilowatt (kW) for newly produced plants between the notes of USD 1,100 to USD 1,400, a dynamic range echoing the diversity of models, markets, and locations. In this financial kaleidoscope, certain burgeoning economies, notably China, India, and the United States, emerge as cost-efficient virtuosos, shaping a narrative where wind energy becomes an accessible symphony. Yet, the financial composition is not a monolithic entity; it is a composition with distinct notes. According to the discerning conclusions of Blanco (2009), various subcomponents wield different weights, each contributing to the financial melody in unique ways. In the context of onshore projects, as articulated in Table 2, the initial ensemble includes components beyond the wind turbine, their contributions harmonizing to form a symphony of capital costs where each element moves to its unique measure, contributing between 18% and 32% to the overarching financial crescendo. In this groundbreaking exploration, capital costs transcend mere financial metrics; they become a financial canvas, painting the portrait of a wind-powered future where the initial investment sets the stage for a sustainable and melodious journey into the heart of energy transformation.

There are various categories into which capital expenses for wind projects can be separated:

- The cost of the actual turbine (factory), which includes production, transformers, propellers, delivery to the site, and installation.

Table 2. Cost model for onshore wind turbine components

Type	Cost model (USD)
Mechanical system	
Bald	$(0.4019r^3 + 2.7445r^{2.5025} - 955.24)/0.6$
Gearbox	$18.1P_r^{1.249}$
Low speed shaft	$0.011 \times (2r)^{2.887}$
Main bearing	$(0.712r/75 - 0.01177) \times (2r)^{2.5}$
Mechanical break	$2.188P_r - 0.1255$
Electrical system	
Generator	$65P_r \times (1 + h_{alt}/15{,}000)$
Power convertor	$49P_r \times (1 + h_{alt}/15{,}000)$
Electrical connection	$45P_r$
Control system	
Pitch system	$0.45 \times (2r)^{2.6578}$
Yaw system	$0.0678 \times (2r)^{2.964}$
Control safety system	50,000
Auxiliary system	
Cooling system	$12P_r \times (1 + h_{alt}/15{,}000)$
Hub	$2 \times (2r)^{2.53} + 24{,}141.275$
Nose cone	$206.69r - 2{,}899.185$
Mainframe	$11.917 \times (2r)^{1.953}$
Nacelle cover	$11.537P_r + 3{,}849.7$
Tower	$0.59595\pi r^2 h - 2{,}121$
Infrastructure	
Foundation	$303.24 \times (\pi h r^2)^{0.4037}$
Roads civil work	$P_r(2.17 \times 10^{-6}P_r^2 - 0.0145P_r + 69.54) \times (1 + h_{alt}/15{,}000)$
Interface connections	$P_r(3.49 \times 10^{-6}P_r^2 - 0.0221P_r + 109.7)$
Engineering permits	$P_r(9.9 \times 10^{-4}P_r + 20.31)$
Transportation	$P_r(1.581 \times 10^{-5}P_r^2 - 0.0375P_r + 54.7) \times (1 + h_{alt}/15{,}000)$
Installation	$1.965 \times (2hr)^{1.1736}(1 + h_{alt}/15{,}000)$

Source: Data from Song et al. (2020).
Note: r is the wind turbine's radius and P_r is its rated power, h is the hub height and h_{alt} is the height from sea level.

- The cost of securing a link to the grid, which includes the installation of cables, substations, connectors, and energy evacuation systems (where they are specially connected to and created for the wind farm).
- The expense of building foundations, roads, and other civil engineering projects.
- Other capital expenses, such as design and engineering fees, consulting and licensing fees, SCADA (monitoring, control, and data acquisition) systems, and monitoring systems.

Harmonizing the Financial Score: Variable Costs

In the grand symphony of renewable energy, wind turbines stand as virtuosos, rendering a melody that resonates with the promise of environmental sustainability. This section unravels the nuanced composition of variable costs, a key movement within the economic score of wind energy projects. In the intricate orchestration of variable costs, operation and maintenance (O&M) emerges as the maestro, commanding a substantial portion of the annual financial performance. While wind turbines, heralding a cost-effective alternative to fossil fuel counterparts, perform elegantly across the economic stage, the substantial shadow of O&M looms large. A tableau of expenditures crucial to shaping the financial dynamics of wind energy projects was presented by Blanco (2009).

As we traverse the crescendo of technological evolution, the study unveils a captivating revelation: larger, modern wind turbine designs, akin to virtuoso performers, demand less O&M than their predecessors. Yet, the composition introduces novel complexities, as these colossal designs bring forth heightened hazards and increased material costs. In this symphonic narrative, the rise in O&M expenditures, including component repair, monitoring, and insurance, becomes a compelling counterpoint. The study's findings, akin to a climactic chord, disclose the financial notes of O&M expenses for projects entering commercial operation between 2015 and 2018. The spectrum, ranging between USD 33 and USD 59 per kilowatt per year, paints a vivid portrait of the financial dynamics. A resonant average of USD 3 per kilowatt per year takes center stage as the total levelized operation cost a harmonic convergence of financial sustainability (Stehly et al. 2020). In this groundbreaking exploration, wind turbine variable costs metamorphose into a symphony of sustainability, where each note played by O&M, component repair, and monitoring resonates with the promise of a renewable energy future.

Illuminating Pathways: Navigating the Economic Evaluation Horizon

In the kaleidoscope of energy investment, economic evaluation serves as the compass, guiding the journey through diverse technological landscapes. This section unfolds as a radiant beacon, shedding light on the methodologies that illuminate the economic efficiency of various energy investments, a crucial paradigm for informed decision-making across the energy spectrum.

Within the expansive terrain of the energy community, where investments in technology resonate as pivotal choices, a set of guiding principles is essential. Economic efficiency, the lodestar for such decisions, finds its articulation through a repertoire of assessment techniques. As we embark on this exploration, a mosaic of closely related and often-utilized methods comes into view, each offering a unique lens to scrutinize economic performance. At the heart of this economic odyssey stands the net present value (NPV) approach—an intricate calculation that harmonizes the temporal dimension of costs and benefits. By discounting all sums for their time value, NPV unfurls as a powerful arbiter, determining the surplus of benefits over costs. The calculation, depicted in the annals of scholarly discourse (Al-Dousari et al. 2019; Muche et al. 2016), serves as a compass, guiding decision-makers through the intricate maze of economic evaluation.

In this illuminating journey through economic evaluation, disparate investments in energy supply or efficiency converge under the unified banner of NPV. The calculation, akin to a celestial navigation tool, empowers decision-makers to discern the economic constellations, facilitating choices that resonate with enduring efficiency and sustainability. As we tread upon the economic evaluation horizon, the NPV approach emerges not merely as a calculation but as a guiding star, navigating the path toward informed and economically sound energy decisions

$$\text{NPV} = \sum_{T=0}^{N} \frac{B_T - C_T}{(1+d)^T} \tag{21}$$

where B_T = benefits in year T; C_T = costs in year T; d = discount rate; and NPV = present value benefits (savings) minus present value costs.

The value needed to cover all expenditures and make a respectable return is known as the LCOE. Future revenues are discounted at a rate that is equivalent to the opportunity cost of capital, or the rate of return that may be earned on other investments with comparable risk, in order to secure a profit. The following equation can be used to express this (Al-Dousari et al. 2019; Perkin et al. 2015):

$$\sum_{t=1}^{t=n} \frac{\text{LCOE} * Q_t}{(1+\dot{d})^t} = \sum_{t=0}^{t=n} \frac{c_t}{(1+\acute{d})^t} \tag{22}$$

where n = period of analysis; Q_t = produced energy; C_t = cost incurred in period t; $\dot{d}$ = discount rate used to future expenditures to return them to their present value; and $\acute{d}$ = discount rate that we assume zero.

Benefits over costs are divided by BCR method. In instance, for an investment to be deemed economically efficient, a value higher than 1 is often necessary. The following formula is used to determine the ratio (Himri et al. 2020):

$$\text{BCR} = \frac{\sum_{T=0}^{N}(CS_T(1+d)^t)}{\sum_{t=0}^{n}(I_T(1+d)^t)} \tag{23}$$

where BCR = savings-to-investment ratio; CS_T = cost savings; and I_T = additional investment costs.

The IRR technique is utilized to determine the discount rate that results in the equivalence of dollar savings and expenses during the study period, leading to an NPV of zero. This discount rate is then used to calculate the return on investment. Typically, the rate of return is determined through a trial-and-error process using the NPV formula, which involves applying various compound interest rates to discount future cash flows until a rate is identified at which the investment's NPV is zero. In the case of a positive NPV, the IRR exceeds the trial rate; in the case of a negative NPV, the IRR falls short of the trial rate.

Emission Chronicles: Charting the Course for a Sustainable Horizon

Amidst the urgent imperative to curtail the global temperature rise and usher in a worldwide energy revolution, this section emerges as a crucible for evaluating the environmental impact through the prism of greenhouse gas emissions. The clarion call of the Paris Agreement reverberates, steering the energy industry toward uncharted territories, yet to be fully navigated by current projections (Gielen et al. 2019).

Pract. Period. Struct. Des. Constr., 2024, 29(3): 04024028

Table 3. GHG emissions intensity of a wind farm and of other types of electricity generation in China, 2019

Type of electricity	GHG emissions intensity (g co_2 eq./kwh)
Wind energy	16.4–28.2
Nuclear energy	10.9–13.9
Hydropower energy	3.1–3.9
Thermal energy	810.0–820.0
Biomass energy	206
Photovoltaic energy	16.0–40.0

Source: Data from Li et al. (2020).

Within the sweeping narrative of climate responsibility, where the imperative is to keep the global surface temperature increase below the pivotal 2°C mark, renewable energy stands as a formidable ally. In 2017, these sustainable sources etched their presence, contributing a quarter to the world's power. Yet, the pace of this transformative change demands acceleration, and the energy industry finds itself at the cusp of a paradigm shift. This section delves into the intricate tapestry of greenhouse gas emissions, unraveling the environmental implications embedded in energy choices. As the world grapples with the challenge of aligning with climate goals, a meticulous examination of emission patterns becomes imperative. The Paris Agreement, a lodestar for this journey, casts its shadow over the energy landscape, signaling an uncharted trajectory. In the alchemy of environmental evaluation, this section transcends the conventional, seeking not just to understand the status quo but to illuminate pathways for a swifter metamorphosis. The evaluation of greenhouse gas emissions becomes more than a statistical exercise; it becomes a testament to our commitment to a sustainable, resilient future (Table 3).

As the world's energy narrative unfolds, this section stands as a testament to the imperative of understanding and mitigating the environmental consequences of our energy choices, laying the groundwork for a greener and more sustainable tomorrow.

Results and Winds of Change: Unraveling the Atmospheric Tapestry

Embarking on a voyage into the heart of wind energy dynamics, this section unfurls the results and discussions arising from a meticulous assessment steeped in NASA's 4-year hourly data. The narrative unfolds, bridging the realms of averages and the robust Weibull distribution to weave a comprehensive understanding of wind energy dynamics. At the outset, the study employs the HOMER software to cast its gaze upon specific horizontal axis wind turbines (HAWT), carefully selected based on power density and the nuanced insights derived from NASA's wind data. The journey delves into the intricacies of power curves, unfurling the tapestry of annual energy production, energy losses, capacity factor, GHG emission reduction, and the economic nuances encapsulated in capital and variable costs.

A Symphony of Wind Speeds

The study opens the curtain on the four-year average wind speeds, a ballet of atmospheric forces choreographed at four different heights. Table 4, an illustrative display, paints the canvas of wind dynamics across diverse topographic terrains. Despite the variations in terrain, each site moves to the sequence of similar wind speeds, a testament to the atmospheric harmony that pervades. As the tale of wind speed unfolds, this section elevates beyond numerical data, offering a narrative that captures the essence of the winds shaping the energy landscape. It sets the stage for a deeper exploration, beckoning the reader to immerse themselves in the atmospheric nuances that underpin the winds of change in the pursuit of sustainable energy. Fig. 4 condenses a comprehensive array of wind-related insights, encompassing monthly variations, yearly trends, and probability distributions. This multifaceted exploration is critical for strategically siting wind energy infrastructure, guaranteeing the optimal utilization of the accessible wind resources. Fig. 4(b) takes center stage, presenting the monthly mean wind speed for Reg at elevations of 10 m, 50 m, 90 m, and 120 m, a captivating average cast over four years. The wind's mellifluous notes resonate at varying heights, with speeds ranging from 3.44–5.66 m/s, 4.88–7.6 m/s, 5.62–8.58 m/s, and 6.03–9.13 m/s, a crescendo of forces ringing the performance of heights.

As the narrative progresses, the dynamics of wind speeds take a prominent position, reaching their peak in June and subsiding to a gentle calm in November. Fig. 4(c), a visual representation of the wind's dynamics, reveals the average wind speeds over a four-year period at various elevations a systematic interplay of 4.33, 5.63, 6.75, and 7.20 m/s. The disparities in average wind speed between 10 m and 50 m, 50 m and 90 m, and 90 m and 120 m become evident, measuring at 37.08%, 13.70%, and 6.76%, respectively.

Within the intricate dynamics of wind patterns, a significant revelation emerges—the ostensibly modest 6.76% variance between 90 m and 120 m conceals substantial power potential. This underscores the nuanced interplay of wind energy, where even a slight variation in velocity can result in profound impacts, resonating with the scientific principles embedded in the cube of velocity.

As the statistical analysis unfolds, Table 4 takes center stage, revealing the detailed interplay of 4-year Weibull parameters (k and c) and standard deviation intricately linked with the average speed. In the chosen expanse of the Reg district, the Weibull parameters manifest with a precision reminiscent of a well-rehearsed ballet, encapsulating the probabilistic nature of wind. Each entry in the table resonances the harmonious interplay of statistical intricacies, setting the stage for the exploration of wind energy potential that awaits further investigation [see Figs. 4(d and e) for similar observations].

Table 5 and Figs. 4(d and e) collectively paint a comprehensive picture of wind speeds at various heights, orchestrated by the Weibull distribution. In this intricate analysis, frequencies align with 10.71%, 11.63%, 13.48%, and 17.38% by guiding winds at 120 m, 90 m, 50 m, and 10 m. The spectrum of wind speeds of 6,

Table 4. Weibull shape and scale parameters, standard deviation and average wind speed annual average for 4-years

	10 m				50 m				90 m				120 m			
Year	SD	k	c	v	SD	k	C	v	SD	k	c	v	SD	K	c	v
2017	2.36	1.91	4.84	4.30	2.98	2.09	6.62	5.87	3.46	2.04	7.51	6.66	3.77	1.99	8.01	7.10
2018	2.22	2.01	4.77	4.22	2.81	2.20	6.56	5.81	3.31	2.12	7.47	6.62	3.63	2.06	7.98	7.07
2019	2.39	1.86	4.77	4.24	3.02	2.03	6.55	5.80	3.50	1.99	7.44	6.59	3.81	1.95	7.93	7.04
2020	2.27	2.13	5.14	4.56	2.86	2.34	7.06	6.26	3.36	2.26	8.04	7.12	3.69	2.19	8.58	7.60
Avg	2.31	1.98	4.88	4.33	2.92	2.17	6.70	5.93	3.41	2.10	7.61	6.75	3.72	2.05	8.13	7.20

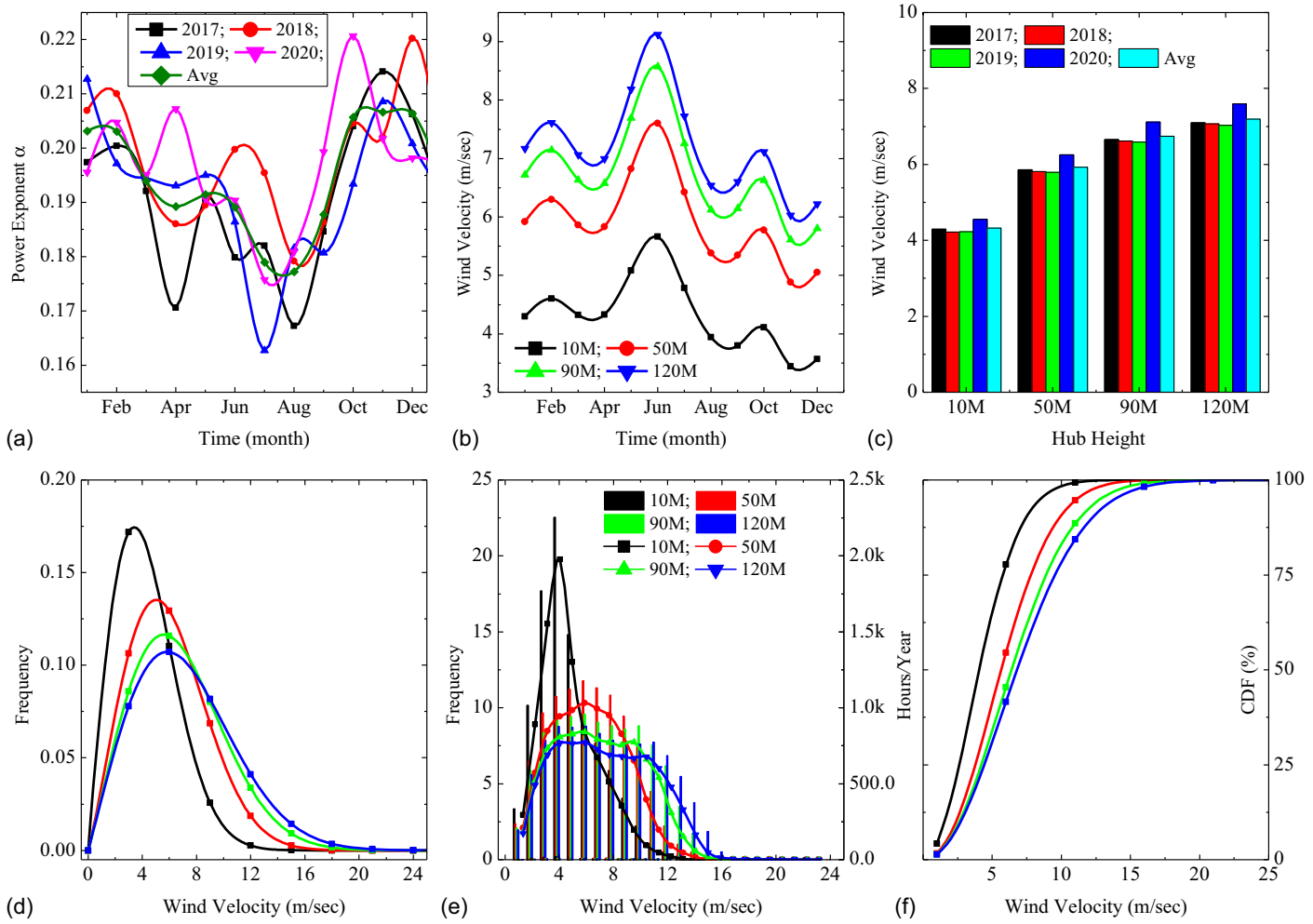

Fig. 4. (a) Average monthly wind speed exponent for 4-years and average of total years; (b) four years monthly average wind speed in different heights; (c) yearly average wind speed in 10, 50, 90, and 120 m heights; (d) wind probability function (PDF) or Weibull distribution function in four heights for site1; (e) wind speed frequency and hours per year in different heights; and (f) wind speed density across four heights cumulatively.

Table 5. Characteristics of wind in Reg

Characteristic	10 m	50 m	90 m	120 m
Standard deviation of wind speed	2.31	2.92	3.41	3.72
Max. hourly wind speed	19.77	23.95	25.69	26.58
Energy pattern factor	1.52	1.39	1.43	1.46
Turbulence intensity	0.53	0.49	0.50	0.52
v_{me}	6.91	9.40	10.72	11.46
v_{mp}	3.42	5.03	5.60	5.86

5.4, 4.8, and 3.2 m/s as each tethered to its corresponding frequency, is notable. Further revelations unfold as winds of 6, 6, 6, and 4 m/s assert their dominance, dictating maximum frequency and hours at 120, 90, 50, and 10 m. Frequencies reverberate of 8.81%, 9.60%, 11.77%, and 22.55% accompanied by the recurring count of 773, 842, 1,032, and 1,977 h, providing a technical ode to the temporal dynamics of wind throughout the seasons. Fig. 4(d) delves into the intricacies of the wind probability function (PDF) or Weibull distribution function for each height, while Fig. 4(e) illuminates the wind speed frequency and hours per year across different heights, further enriching the nuanced understanding of wind behavior. Additionally, Fig. 4(f) elucidates the cumulative wind speed density across the four heights, providing a comprehensive view of the wind distribution across the specified elevations. Together, these elements contribute to a nuanced and comprehensive understanding of the wind characteristics in the studied area.

Embarking on the analysis presented in Fig. 4(f), the cumulative wind speed distribution for Reg unfolds as a detailed account at four distinct heights. The graphic reveals that, during 50.9%, 58.8%, 69.1%, and 79.2% of the year, the wind speeds at 10 m, 50 m, 90 m, and 120 m surpass the 4 m/s threshold. In the context of wind energy, this insight is noteworthy, considering that 4 m/s is often the threshold for many commercial turbines, signifying their effective entry into the realm of power generation. Despite occasional gentle winds, the speeds seldom exceed the turbine cut-out speeds, typically ranging between 20 and 25 m/s. This subtle observation underscores that, in the realm of wind dynamics, managing speed is both an artistic and a practical consideration.

Wind Dynamics and Terrain Interaction

In this integrated exploration, we dissect key elements governing wind behavior and terrain characteristics, offering a comprehensive understanding for civil engineering applications. Our scrutiny begins with an in-depth analysis of surface roughness and its intricate correlation with average wind speeds across different elevations (10, 50, 90, and 120 m). Employing a logarithmic profile (log law)

Pract. Period. Struct. Des. Constr., 2024, 29(3): 04024028

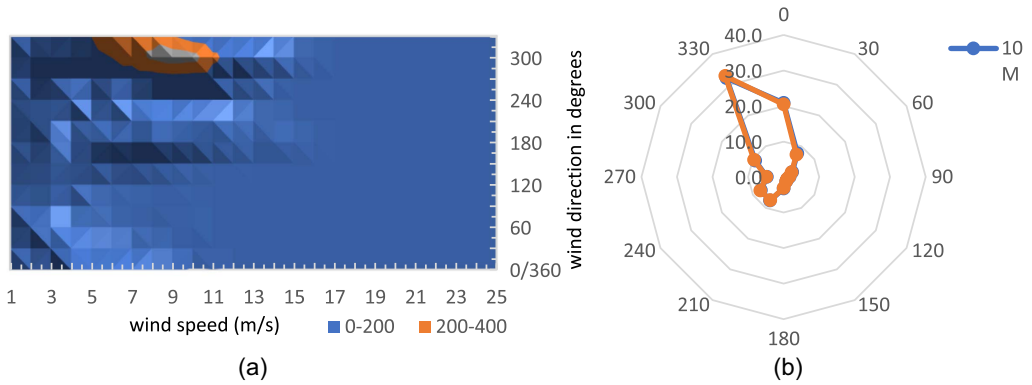

Fig. 5. (a) Wind direction with respect to wind speed and occurring frequency; and (b) wind direction for Reg in 10 M and 50 M.

curve, we unveil the nuanced surface roughness length of the Reg terrain, gracefully oscillating between 128 mm and 130 mm. Navigating the symphony of wind, our focus shifts to understanding the pivotal role of wind direction in selecting optimal wind farm sites. Illustrated through a detailed wind rose (Fig. 5), our analysis orchestrates wind direction frequencies at varying speeds. The winds, following atmospheric patterns, exhibit a prominent movement of floor between 8 and 10 m/s and within the 280°–320° directions, significantly influencing the yearly mean wind directions at 10 m and 50 m, 319.50° and 319.22°, respectively. Delving into the tempest's heart, we illuminate the realm of turbulence intensity, a critical factor shaping wind dynamics. Departing from the tranquility of mean wind speeds, turbulence subtly influences the wind's behavior. At heights of 10 m, 50 m, 90 m, and 120 m, turbulence intensity averages 0.53, 0.49, 0.50, and 0.52, respectively, providing distinct insights into the tempestuous ballet of wind (see Table 5) (Tasneem et al. 2020).

Atmospheric Dynamics and Wind Potential

Embarking on a comprehensive exploration, this section unravels the symphony of atmospheric elements, delving into air dynamics encompassing pressure, temperature, and humidity. Simultaneously, it unveils the intricacies of wind potential, focusing on power and energy densities. This dual-pronged analysis provides a holistic understanding of the environmental conditions shaping wind dynamics and their implications for sustainable energy harnessing in the Reg district.

Embarking on a meticulous exploration of air dynamics, this study taps into NASA's data to unravel the nuanced interplay of relative humidity, pressure, and air temperature. Averaging at 3.87 g/kg, 86.73 kPa, and 20.25°C, respectively, these fundamental parameters serve as the cornerstone for calculating air density. The composition of Earth's breath, meticulously measured at 2 m above ground level, reveals an air density oscillating between 0.979 and 1.082 kg/m^3, culminating in an average of 1.032 kg/m^3. Fig. 6(a), explains the average air density for the selected site. This comprehensive examination of atmospheric elements provides a foundational understanding of the environmental conditions shaping wind dynamics in the Reg district. By dissecting these key variables, the study sets the stage for a detailed analysis of wind potential and its implications for sustainable energy harnessing. The culmination of wind's potential unfolds as we delve into the revelation of power and energy densities. Acting as the unseen conductor, air density takes center stage, guiding the yearly wind power density at four elevations to an orchestrated peak [Fig. 6(b)]. The difference of comparison between measured data and the ethereal Weibull distribution [Fig. 6(d)] exposes a nuanced interplay, particularly highlighting peak powers during June and November. At heights of 10, 50, 90, and 120 m, the annual averages stand at 88.76, 210.24, 315.76, and 392.96 W/m^2 [see Fig. 6(c)]. This interpretation paints an intense depiction of a site intricately merged into the link of wind dynamics, offering a glimpse into a future where power and energy densities converge seamlessly in the symphony of sustainable energy generation. The data underscores the site's harmonious embrace with the winds, reinforcing its potential as a strategic location for wind energy infrastructure. The study transcends the conventional boundaries of wind energy exploration, offering a holistic narrative that goes beyond statistics. Through a meticulous examination of terrain, wind direction dynamics, turbulence intensity, and atmospheric elements, we lay the groundwork for a new era in sustainable energy. The Reg district emerges not only as a geographical location but as a harmonious symphony of wind dynamics, paving the way for transformative advancements in renewable energy and sustainable engineering practices.

Wind Turbines

Ensuring wind turbines adhere to IEC 61400-1_2019 standards is paramount for their reliability and performance. This section provides a detailed discussion on the compliance of 12 wind turbines with these international standards (see Table 6). Each turbine serves as a maestro, contributing to the overall symphony of energy production. The power curves in Fig. 7(a) offer a visual representation of the performance of turbines across different IEC wind classes, from 1a to 3b. Capacity factors, ranging from 23% to 49.5%, act as brilliant performances, highlighting the efficiency of LTW80, E-115, EWT61, V82, G1500, E-53, XANT330, EWT54, VergMP-C, V47, WF45, and WES250. The intricate performance of these turbines in response to varying wind conditions emphasizes the importance of selecting the right turbine for optimal energy production. This concludes by underlining the significance of IEC standards in ensuring the reliability and efficiency of wind turbines.

Efficiency in wind farms is a multifaceted concept, encompassing factors such as turbine spacing, wake effects, and overall energy losses. This section delves into unveiling the impact of turbine placement on energy production and losses. Strategically spacing turbines at 7D distances, where D is the rotor diameter, minimizes wake effects and reduces energy losses to a mere 1.75%. Fig. 7(b) further illustrates a 5% dip in capacity factors, emphasizing the delicate balance between power and efficiency. The meticulous consideration of energy losses and wake effects is pivotal in optimizing the efficiency of wind farms. The observed 5% dip in capacity factors emphasizes the fine balance between maximizing power

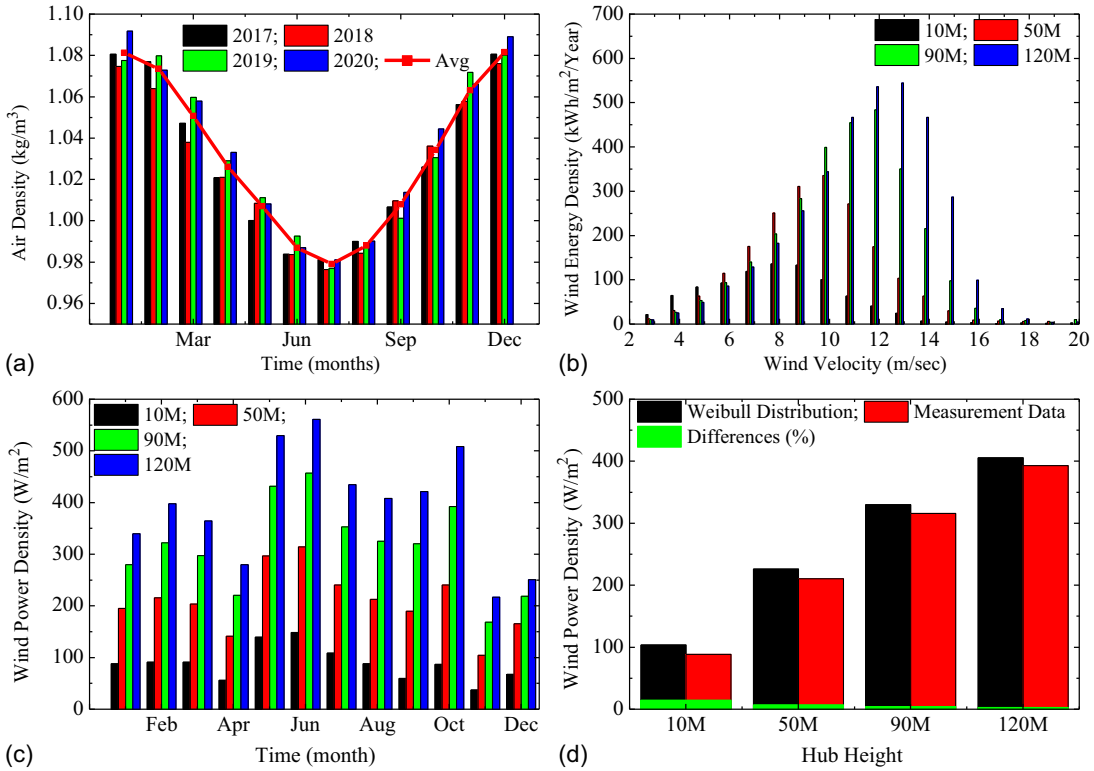

Fig. 6. (a) Monthly air density in 2 m above ground level; (b) annual wind energy density for different speeds using four-year average data; (c) monthly wind power density with monthly average; and (d) annual wind power density using Weibull distribution and measurement data with % difference.

Table 6. Wind turbine descriptions

WT model	Power (rated) P_r (kW)	Diameter of rotor D (m)	Hub height H_{hub} (m)	Wind speed			Swift area (sq.m)	Power density (W/m^2)
				Cut-in v_i (m/s)	Rated v_r (m/s)	Cut-off v_o (m/s)		
E-115	3,000	115.7	122	2	12	25	10,515	285
XANT330	330	33	55	3	13	20	855	386
G1500	1,500	83	80	4	14	25	5,411	277
EWT61	900	60.9	75	3	12	25	2,913	309
E-53	800	52.9	73	2	13	25	2,198	364
LTW80	1,000	80	80	3	11	25	5,027	199
VergMP-C	275	32	55	4	13	25	804	342
V47	660	47	50	4	17	25	1,735	380
WES250	250	30	48	3	13	25	707	354
WF45	500	45	38	5	14	25	1,591	314
v82	1,650	82	70	4	13	25	5,282	312
EWT54	900	54	50	3	14	25	2,290	393

generation and minimizing losses. Efficiency is a critical consideration in wind farm design, and the findings contribute to the ongoing dialogue on optimizing wind farm layouts for improved performance and sustainability. Reducing greenhouse gas emissions is a key objective in transitioning to sustainable energy sources. This study explores the precise impact of wind turbines on greenhouse gas reduction, providing a nuanced understanding of their environmental contribution. The calculated mean value of 22.35 g CO_2/kWh serves as a metric for the environmental impact of wind turbines (see Fig. 8). Contrasted with thermal power plants emitting 815 g CO_2/kWh, wind turbines emerge as virtuosos in reducing greenhouse gases. It is observed that the wind turbines with higher hub heights leverage the benefits of elevated wind resources, resulting in increased energy output and, consequently, a more significant reduction in greenhouse gas emissions.

Cost Analysis: Unraveling the Financial Aspects

This section ventures into an exhaustive exploration of the financial dimensions of wind turbines, seeking to unravel the intricacies governing their economic viability. At the heart of this discussion lies the detailed analysis presented in Fig. 9, a visual masterpiece that intricately examines crucial financial parameters such as capital costs, net present value (NPV), and the cost per kW of power. Understanding the financial landscape of wind turbines necessitates a keen awareness of the capital costs associated with their deployment.

Pract. Period. Struct. Des. Constr., 2024, 29(3): 04024028

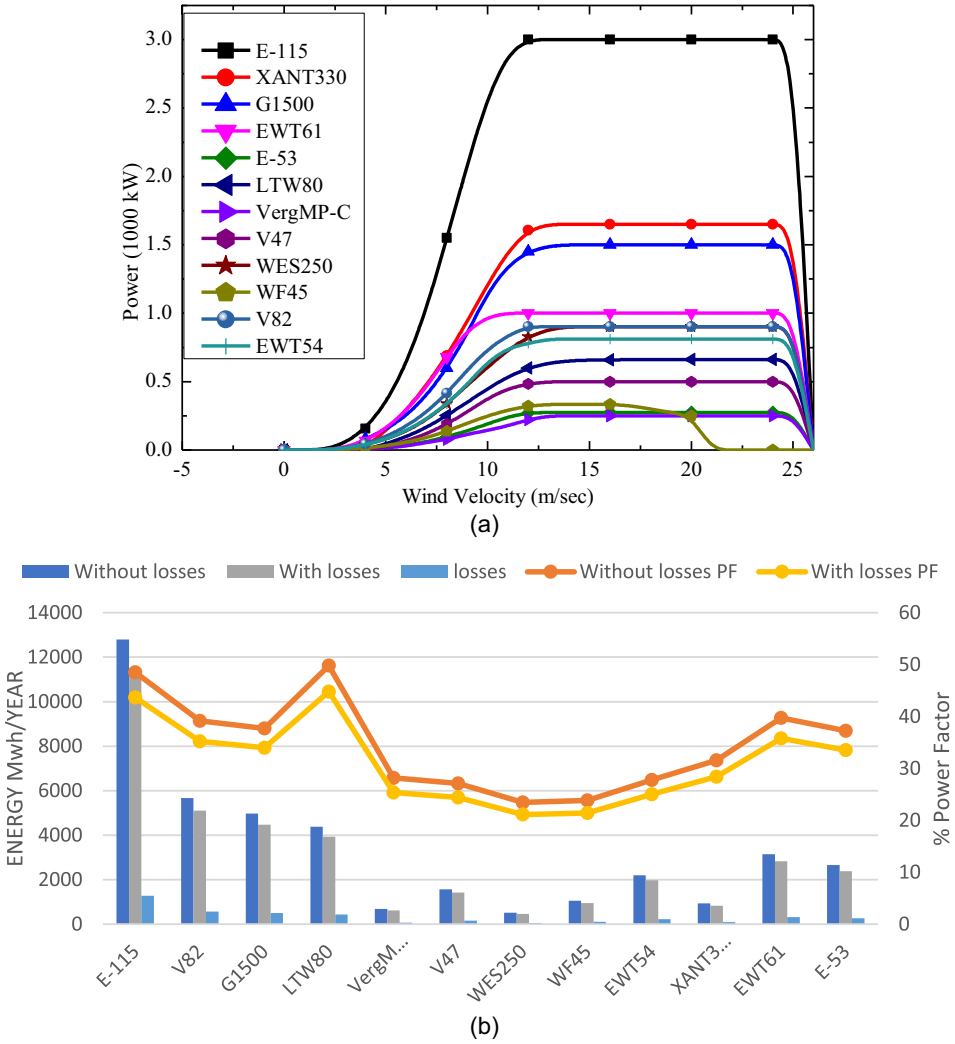

Fig. 7. (a) Power curves for selected wind turbines; and (b) total generated energy and capacity factors per year with and without losses.

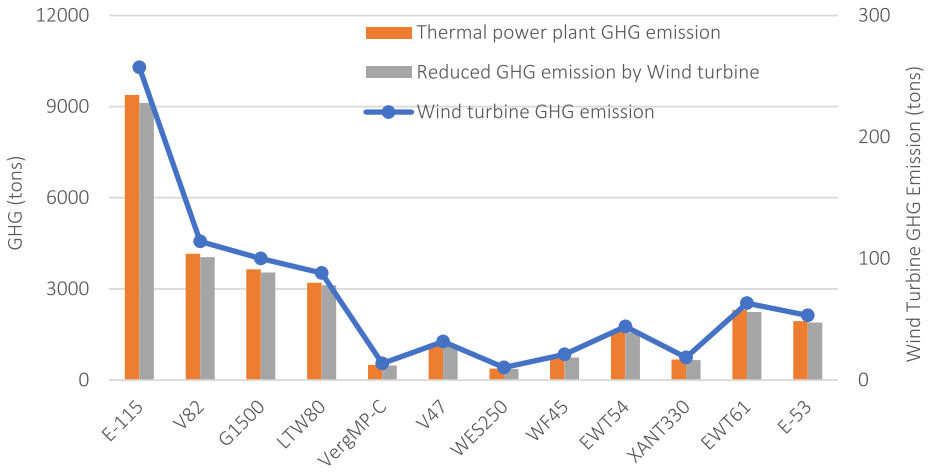

Fig. 8. GHG emission and reduction for wind turbines.

Fig. 9 acts as a guiding compass, breaking down capital costs into mechanical, electrical, control, auxiliary systems, and infrastructure. This granular perspective provides stakeholders with profound insights into the strategic allocation of financial resources within the intricate framework of wind turbine infrastructure. Delving deeper, we uncover the diverse spectrum of capital costs, spanning an eloquent range from USD 828 to USD 1,273 per kW of power. Moving beyond a mere numerical presentation, this discussion

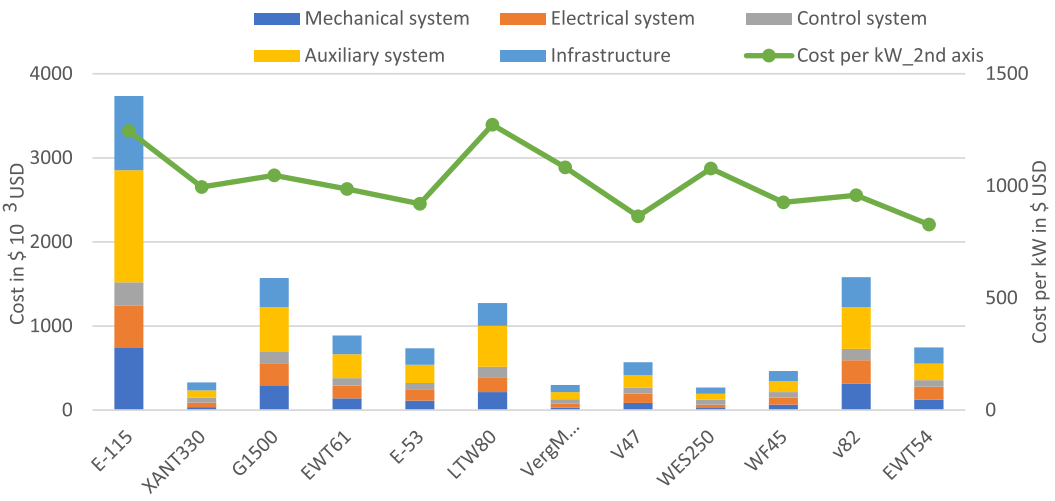

Fig. 9. Capital cost breakdown for each wind turbine and cost of 1 kW power.

contextualizes the range, offering stakeholders a nuanced understanding of the economic implications associated with different turbine options. The spectrum becomes a palette, empowering decision-makers to sculpt their choices based on budgetary considerations and long-term financial objectives. A cornerstone of our financial exploration is the intricate analysis of NPV, a crucial metric for assessing the financial viability of wind turbine projects. Fig. 9 unfolds NPV values ranging from USD 863 to USD 3,737. However, this discussion transcends the presentation of numerical values, delving into a nuanced interpretation that considers potential returns on investment. It engages in a performance with operational costs, maintenance considerations, and the anticipated lifespan of the turbines.

The study descends into the essential metric of cost per kW of power, shining a spotlight on its significance in the economic evaluation of wind turbines. Fig. 9 meticulously captures this parameter, providing a stage for a comparative analysis across diverse turbine options. Stakeholders can gauge the efficiency and economic feasibility of each turbine model by examining the cost per unit of power generated. As the financial symphony of wind turbines unfolds, the implications for the future of sustainable energy become pronounced. The careful consideration of capital costs, NPV, and cost per kW not only guides current decisions but shapes the trajectory of wind energy innovations. The spectrum of costs presented in Fig. 9 offers a dynamic landscape for future research and development, encouraging the exploration of more cost-effective and efficient turbine options. This study concludes by emphasizing the indispensable need for a holistic comprehension of the financial landscape in the wind energy sector. Fig. 9 serves not merely as a set of figures but as a valuable resource, guiding industry professionals, researchers, and policymakers in navigating the economic intricacies of wind turbine deployment. As we unravel the economic symphony of wind turbines, we envision a future where sustainability and financial prudence converge in a harmonious crescendo, propelling the wind energy sector into new realms of innovation and viability.

The NPV method, while an invaluable tool for system design, scaling, and investment decisions, encounters limitations when applied to assets offering different services (see Table 7). In the context of this analysis, where the tariff of energy is pegged at 8 cents per kWh, NPV unfolds as a critical metric. Notably, LTW80 and E-115 wind turbines emerge as economic stalwarts, boasting maximum NPVs of USD 3,737 and USD 3,619 per kW of power, respectively. In contrast, the WES250 wind turbine presents the lowest NPV at USD 863 per kW of power. The selection of the E-115 wind turbine for the wind power plant design is justified by its high-power density per swift area, coupled with a smaller footprint compared to the LTW80.

LCOE, a pivotal metric in the economic evaluation of wind turbines, paints a vivid picture of the cost per unit of energy. Among the 12 wind turbine types analyzed, the E-115 and LTW80 models exhibit the lowest LCOE at USD 0.0328 and USD 0.0356, respectively (see Table 8).

This data positions them as economically efficient choices for sustainable energy production. The BCRs further strengthen the economic case for wind energy investments. LTW80 and E-115, with BCRs of 3.35 and 3.31, respectively, underscore their close economic viability. However, the decision to favor the E-115 over the LTW80 aligns with the specificities of the capital cost model designed for a 2.8MW wind turbine in a 200MW wind farm reference project. Diving into the internal rates of return (IRR) provides a nuanced view of the financial vibrancy of selected wind turbines. WES250 exhibits the lowest IRR, while LTW80, V82, E-53, E-115, and ETW61 showcase the highest IRRs, with a marginal 0.25% difference among them. The calculation of payback periods, accounting for the time value of money with a 2.5% annual inflation rate, complements the economic analysis. Table 9 lays out payback periods, offering insights into the recovery timeframe if the tariff on energy remains at USD 0.08. Beyond the initial investment recovery, subsequent years witness the calculation of benefits, net profit, and variable costs, providing a comprehensive financial outlook. Zooming out to the macro perspective, the selected site's average area of approximately 360 km^2 is poised for substantial power production. Leveraging the E-115 wind turbine, a 60 MW wind farm design emerges as the optimal choice. This decision is grounded in a

Table 7. The primary financial metrics for cost breakdown

Parameter	Amount	Units	References
Average cost of energy in KDR	0.080	USD/kWh	This study
Average inflation rate	2.5	%	Himri et al. (2020)
Discount rate	12	%	Himri et al. (2020)
Project life	25	Years	This study
Operation and maintenance cost	33–59	USD/kW/year	Stehly et al. (2020)

Table 8. Economic analysis of all wind turbines

Turbine model	SPP (years)	LCOE (USD)	NPV (USD 10^3)	NPV/kW (USD/kW)	BCR	IRR (%)	Cost of 1 kW (USD)
E-115	4.85	0.0328	10,857.58	3,619.19	3.31	26.83	1,244.86
XANT330	6.44	0.0444	641.34	1,943.46	2.45	18.79	994.74
G1500	5.52	0.0386	3,834.81	2,556.54	2.81	22.79	1,047.61
ETW61	4.88	0.0356	2,568.23	2,853.59	3.05	26.70	986.27
E-53	4.85	0.0363	2,146.64	2,683.30	2.99	26.89	920.77
LTW80	4.82	0.0324	3,737.12	3,737.12	3.35	27.08	1,272.81
VergMP-C	8.27	0.0526	387.51	1,409.13	2.07	13.61	1,082.77
V47	6.96	0.0491	990.79	1,501.20	2.21	17.04	864.99
WES250	10.60	0.0630	215.74	862.95	1.72	9.64	1,077.61
WF45	8.91	0.0577	528.67	1,057.35	1.88	12.35	926.17
V82	4.83	0.0357	4,637.33	2,810.50	3.04	27.04	958.86
EWT54	6.44	0.0470	1,457.30	1,619.22	2.31	18.81	827.70

strategic alignment with low LCOE, favorable payback years, and a comparatively higher power density per swift area of the turbine. In conclusion, this economic exploration transcends traditional metrics, delving into a holistic understanding of wind energy investments. Beyond NPV, the interplay of LCOE, BCR, IRR, and payback periods guides stakeholders toward economically feasible and sustainable wind energy solutions. The intricate performance of these metrics coordinates a symphony of decision-making, paving the way for a greener and economically vibrant future in wind energy utilization.

Optimizing Wind Turbine Array Spacing: A Technological Odyssey

The intricate movement of wind turbines within a wind farm creates a technological tapestry laden with challenges, and array spacing emerges as a critical choreographer in this ballet. Wind turbine placement, often referred to as wind turbine array spacing, becomes a pivotal consideration in maximizing energy extraction and minimizing inefficiencies. The technological nuances extend beyond the physical dimensions of the turbines, intertwining with terrain effects and wake effects.

Terrain effects, stemming from the undulating landscape, introduce variations in wind resources that demand meticulous attention when orchestrating the placement of turbines. The optimal positioning of turbines within a wind farm necessitates a comprehensive understanding of these terrain effects to ensure a harmonious energy extraction.

The wake effect, a phenomenon where upwind turbines impact the wind speeds at downwind turbines, introduces a layer of complexity. This turbulence can lead to a reduction in energy output and heightened wear and tear on downwind turbines. The intricacies of array spacing play a crucial role in mitigating these effects, striking a balance between maximizing energy yield and minimizing wake-induced losses.

In the heart of this technological ballet stands a wind farm powered by twenty E-115 wind turbines, strategically arranged in four rows and five columns. The turbines, oriented at 319.5°north, harness the flat and arid landscape of the Reg district. Each turbine, with a diameter of 115.7 m, elegantly occupies 0.281116 km^2 in both 3D and 7D distances.

The total covered area of the wind farm, a sprawling 5.622336 km^2, becomes the canvas for energy production, meticulously designed to harness the relentless winds of the region. The site's flat and arid characteristics, coupled with its proximity to the district center, add to the logistical efficiency of the wind farm.

Through meticulous analysis and design, the wind farm achieves an annual net energy production of 230,250.67 MWh with an impressive 43.69% capacity factor. However, this achievement is not without its losses. Wake effects, downtime, airfoil soiling, miscellaneous factors, and adjustments for pressure and temperature introduce a 10% loss, amounting to 25,583.41 MWh. These losses, meticulously calculated using Table 2, underscore the importance of technological precision in wind farm design.

Despite the Reg district's modest population of 7,752, the wind farm's energy production dwarf's local demand. With an average energy consumption per capita in Afghanistan at 145 kWh/year, the wind farm's potential extends beyond serving the local community. It emerges as a strategic contributor to the national grid and the energy needs of Kandahar city.

Table 9. Capital cost breakdown for 60MW wind farm with twenty E-115 wind turbines

Type of cost	Wind farm capital costs in million USD
Mechanical system	
Blade	4.91
Gearbox	7.97
Low speed shaft	0.20
Main bearing	1.55
Mechanical break	0.13
Electrical system	
Generator	4.24
Power convertor	3.20
Electrical connection	2.70
Control system	—
Pitch system	2.74
Yaw system	1.77
Control safety system	1.00
Auxiliary system	
Cooling system	0.78
Hub	7.12
Nose cone	0.18
Mainframe	2.55
Nacelle cover	0.77
Tower	15.25
Infrastructure	—
Foundation	1.77
Roads civil work	1.28
Interface connections	4.49
Engineering permits	1.40
Transportation	5.51
Installation	3.17
Sum	74.69

Table 10. Important variables for cost calculations

Some important variables for costs	Value
Wind turbine model	Model E-115
Radius of wind turbine (m)	57.85
Rated power of wind turbine (kW)	3,000
Average altitude of site from Sea level (m)	1,316
Hub height of wind turbine (m)	122
Variable cost (USD/kW/year)	43
Annual inflation rate (%)	2.5
Number of wind turbines	20
Average Afghanistan grid electricity tariff in 2021 (USD/kWh)	0.08

Table 11. Economic analysis of all wind turbines and wind farm

Economic factors	Value
Number of Model E-155 turbines	20
SPP (years)	4.85
LCOE (USD)	0.0328
NPV (USD 10^3)	217,151.7
NPV/kW (USD /kW)	3,619.19
BCR	3.31
IRR (%)	26.83
Cost of 1 kW (USD)	1,244.86

The financial underpinning of this technological marvel involves capital costs, meticulously calculated using equations from Table 2 and given in Table 9. The mechanical, electrical, control and auxiliary systems, and infrastructure costs sum up to USD 74.69 million for the twenty E-115 wind turbines (see Table 10). These capital costs, coupled with variable costs accounting for rent, insurance, service and spare parts, power from the grid, miscellaneous costs, and administration costs, create a robust economic framework.

The economic analysis, presented in Table 11, reflects a total present cost value of USD 122.23 million and a total present benefits value of USD 339.38 million. This translates to a robust NPV of USD 217.15 million, firmly in positive territory. The wind farm's economic resilience further manifests in a short payback period of 4.85 years, coupled with a high internal rate of return of 27.4%.

The financial symphony extends to NPV per kW at USD 3,619, a BCR of 3.3084, and a cost of one kW power at USD 1,244.86. The LCOE, a key metric for economic feasibility, stands at 3.28 cents, aligning favorably with other resources available in Kandahar.

Beyond the economic spotlight, the wind farm's environmental footprint shines. The wind turbines, with an average greenhouse gas emission of 22.35 g/kWh, become ecological maestros. Reg wind farm's annual emissions of 5,146 tons, and a total of 128,652 tons over its 25-year life, contrast starkly with the emissions of a thermal power plant producing the same energy. A thermal plant could emit about 187,654 tons per year, totaling 4,691,357 tons over 25 years. The wind farm, by reducing GHG emissions by 182,508 tons per year (or about 97.26%), emerges as a potent force in the fight against climate change.

In conclusion, the wind farm in the Reg district transcends technological challenges, showcasing a harmonious performance of economic viability, environmental responsibility, and energy abundance. It stands not merely as a collection of turbines but as a technological symphony contributing to the broader narrative of sustainable energy.

Conclusion and Policy Implications

The structural safety analysis in this study is crucial for ensuring the resilience of selected wind turbines. Survival wind speeds, with a cutoff at 25 m/s and a design consideration for 50 m/s, highlight the turbines' capacity to withstand extreme conditions. Examining different configurations, the E-115 design optimizes for moderate winds, while the VergMP-C design is robust for higher speeds. This analysis contributes vital insights to ensure the structural soundness and resilience of wind turbines across diverse environmental conditions.

Drawing insights from a comprehensive four-year data set, this study intricately deciphers the wind dynamics of the Reg region, laying the groundwork for informed decisions in wind energy deployment. The average wind speed exponent of 0.194395 and a terrain roughness length of 128–130 mm emerge as critical parameters, providing a nuanced understanding of the wind resource landscape.

The temporal variability in wind speeds, detailed across various heights, underscores the dynamic nature of the wind regime in Reg. The yearly average wind speeds at 10, 50, 90, and 120 m reveal a progressive increase, signifying the potential for harnessing stronger winds at greater heights. The windiest months, June and November, spotlight the temporal nuances that must be considered in wind farm planning.

Weibull distributions unravel the frequency of different wind speeds, with the highest wind frequencies identified at 6, 5.4, 4.8, and 3.2 m/s. This granular understanding of wind speed distributions serves as a valuable tool in optimizing turbine design and placement.

The capacity factors of selected wind turbine models, ranging from 23% to 49.5%, become a key metric in evaluating their efficiency. Capital costs, varying from USD 828 to USD 1,273 per kW of power, depict the economic landscape of different turbine options. The EWT54 model stands out with the lowest capital cost per kW, while the LTW80 model holds the highest.

The culmination of these insights finds its embodiment in the design of a wind farm powered by twenty E-115 wind turbines. The arrangement, with meticulous attention to spacing and orientation, spans a flat and arid area of approximately 360 km^2 in the Reg region. The wind farm's annual net energy production of 230,250.67 MWh, coupled with a robust capacity factor of 43.69%, positions it as a significant contributor to the energy landscape.

The economic viability, a cornerstone of wind energy projects, is encapsulated in the financial symphony orchestrated by the wind farm. Capital costs, distributed across mechanical, electrical, control, auxiliary systems, and infrastructure, sum up to USD 74.69 million. The average variable cost, at USD 43 per kW per year, contributes to the economic tapestry.

The economic analysis, reflected in a NPV of USD 217.15 million, a short payback period of 4.85 years, and a commendable internal rate of return (IRR) of 27.4%, accentuates the project's financial resilience. The wind farm emerges not only as an energy powerhouse but as a sound financial investment.

The environmental impact of the wind farm adds a layer of sustainability to its narrative. With an average greenhouse gas emission of 22.35 g/kWh, the wind farm becomes a formidable force in mitigating climate change. The reduction of 182,508 tons of greenhouse gases annually, compared to a thermal power plant, exemplifies the environmental conscientiousness of wind energy.

The conclusion draws attention to the policy implications embedded in this study. The Reg region, with its favorable wind resource and economic feasibility, calls for a strategic policy framework to encourage and facilitate the expansion of utility-scale wind

farms. Policymakers can leverage the insights from this study to craft regulations that incentivize the adoption of wind energy, promoting a sustainable and resilient energy future for the region.

In considering future research directions, it would be valuable to delve into more localized wind flow patterns and micro-siting strategies to optimize turbine placement further. Additionally, investigating the integration of advanced technologies, such as machine learning algorithms, for enhanced wind resource assessment could offer promising avenues for future exploration.

Despite the comprehensive nature of this study, there are certain limitations. The data set's temporal scope, spanning four years, may not capture longer-term variations in wind patterns. Moreover, the study assumes a static wind turbine efficiency, and future research could explore dynamic efficiency models that consider real-time operational conditions. Addressing these limitations will contribute to a more robust understanding of wind energy dynamics in the Reg region.

Data Availability Statement

All data, models, and code generated or used during the study appear in the published article.

References

Abbes, M., and J. Belhadj. 2012. "Wind resource estimation and wind park design in El-Kef region, Tunisia." *Energy* 40 (1): 348–357. https://doi.org/10.1016/j.energy.2012.01.061.

Abbes, M., and J. Belhadj. 2014. "Development of a methodology for wind energy estimation and wind park design." *J. Renewable Sustainable Energy* 6 (5): 53103. https://doi.org/10.1063/1.4895919.

Adaramola, M. S., M. Agelin-chaab, and S. S. Paul. 2015. "Assessment of wind power generation along the coast of Ghana." *Energy Convers. Manage.* 77 (2014): 61–69. https://doi.org/10.1016/j.enconman.2013.09.005.

Afanasyeva, S., J. Saari, M. Kalkofen, J. Partanen, and O. Pyrhönen. 2016. "Technical, economic and uncertainty modelling of a wind farm project." *Energy Convers. Manage.* 107 (Feb): 22–33. https://doi.org/10.1016/j.enconman.2015.09.048.

Ahmad, S. S., A. Al Rashid, S. A Raza, A. A. Zaidi, S. Z. Khan, and M. Koç. 2022. "Feasibility analysis of wind energy potential along the coastline of Pakistan." *Ain Shams Eng. J.* 13 (1): 101542. https://doi.org/10.1016/j.asej.2021.07.001.

Al-Dousari, A., W. Al-Nassar, A. Al-Hemoud, A. Alsaleh, A. Ramadan, N. Al-Dousari, and M. Ahmed. 2019. "Solar and wind energy: Challenges and solutions in desert regions." *Energy* 176 (Jun): 184–194. https://doi.org/10.1016/j.energy.2019.03.180.

Alfawzan, F., J. E. Alleman, and C. R. Rehmann. 2020. "Wind energy assessment for NEOM city, Saudi Arabia." *Energy Sci. Eng.* 8 (3): 755–767. https://doi.org/10.1002/ese3.548.

Anwarzai, M. A., and K. Nagasaka. 2014. "A Research and Development of Wind Energy for Afghanistan Research on development of renewable energies for Afghanistan View project Renewable Energy Surplus Power Management View project." Accessed April 10, 2023. http://www.epa.gov/oswercpa/docs/wind_decision_tree.pdf.

Bahrami, A., A. Teimourian, C. Onyeka, and N. Khosravi. 2019. "Assessing the feasibility of wind energy as a power source in Turkmenistan; a major opportunity for Central Asia's energy market." *Energy* 183 (Aug): 415–427. https://doi.org/10.1016/j.energy.2019.06.108.

Blanco, I. 2009. "The economics of wind energy." *Renewable Sustainable Energy Rev.* 13 (6–7): 1372–1382. https://doi.org/10.1016/j.rser.2008.09.004.

Chadee, X. T., and R. M. Clarke. 2018. "Wind resources and the levelized cost of wind generated electricity in the Caribbean islands of Trinidad and Tobago." *Renewable Sustainable Energy Rev.* 81 (Jan): 2526–2540. https://doi.org/10.1016/j.rser.2017.06.059.

Davis, N. N., et al. 2023. "Ray Drummond; The global wind atlas: A high-resolution dataset of climatologies and associated web-based application." *Bull. Am. Meteorol. Soc.* 104 (8): E1507–E1525. https://doi.org/10.1175/BAMS-D-21-0075.1.

Earnest, J., and S. Rachel. 2019. *Wind power technology.* 3rd ed. New Delhi, India: PHI Learning Private.

Elias, S. 2024. "Vibration improvement of offshore wind turbines under multiple hazards." In Vol. 59 of *Structures*, 105800. Amsterdam, Netherlands: Elsevier.

Elliott, D. 2011. *Wind Resource Assessment and Mapping for Afghanistan and Pakistan*. Golden, CO: National Renewable Energy Lab.

Eltamaly, A. M. 2013. "Design and implementation of wind energy system in Saudi Arabia." *Renewable Energy* 60 (Feb): 42–52. https://doi.org/10.1016/j.renene.2013.04.006.

Feng, J., and W. Z. Shen. 2017. "Design optimization of offshore wind farms with multiple types of wind turbines." *Appl. Energy* 205 (Apr): 1283–1297. https://doi.org/10.1016/j.apenergy.2017.08.107.

Gaur, S., S. Elias, T. Höbbel, V. A. Matsagar, and K. Thiele. 2020. "Tuned mass dampers in wind response control of wind turbine with soil-structure interaction." *Soil Dyn. Earthquake Eng.* 132 (Apr): 106071. https://doi.org/10.1016/j.soildyn.2020.106071.

Gielen, D., F. Boshell, D. Saygin, M. D. Bazilian, N. Wagner, and R. Gorini. 2019. "The role of renewable energy in the global energy transformation." *Energy Strategy Rev.* 24 (Jan): 38–50. https://doi.org/10.1016/j.esr.2019.01.006.

Gökçek, M., and M. Serdar. 2009. "Evaluation of electricity generation and energy cost of wind energy conversion systems (WECSs) in Central Turkey." *Appl. Energy* 86 (12): 2731–2739. https://doi.org/10.1016/j.apenergy.2009.03.025.

González, J. S., Á. G. G. Rodríguez, J. C. Mora, M. B. Payán, and J. R. Santos. 2011. "Overall design optimization of wind farms." *Renewable Energy* 36 (7): 1973–1982. https://doi.org/10.1016/j.renene.2010.10.034.

Himri, Y., M. Merzouk, N. K. Merzouk, and S. Himri. 2020. "Potential and economic feasibility of wind energy in South West region of Algeria." *Sustainable Energy Technol. Assess.* 38(Oct): 100643. https://doi.org/10.1016/j.seta.2020.100643.

Ibrahim, M. Z., and A. Albani. 2016. "Wind turbine rank method for a wind park scenario." *World J. Eng.* 13 (6): 500–508. https://doi.org/10.1108/WJE-09-2016-0083.

IRENA. 2018. *Energy profile*. Kabul, Afghanistan: Ministry of Energy and Water.

Irshad, A. S. 2023. "Design and comparative analysis of grid-connected BIPV system with monocrystalline silicon and polycrystalline silicon in Kandahar climate." *MATEC Web Conf.* 374 (Aug): 03002. https://doi.org/10.1051/matecconf/202337403002.

Irshad, A. S., and A. G. Noori. 2022. "Evaluating the effects of passive cooling and heating techniques on building energy consumption in Kandahar using CLTD method." *Mater. Today Proc.* 57 (Aug): 595–602. https://doi.org/10.1016/j.matpr.2022.01.456.

Jung, C., and D. Schindler. 2019. "The role of air density in wind energy assessment–A case study from Germany." *Energy* 171 (Apr): 385–392. https://doi.org/10.1016/j.energy.2019.01.041.

Kalogirou, A. 2014. *Solar energy engineering processes and systems*. 2nd ed. Millbrae, CA: Academic Press.

Katsigiannis, Y. A., G. S. Stavrakakis, and C. Pharconides. 2013. "Effect of wind turbine classes on the electricity production of wind farms in Cyprus Island." In Vol. 2013 of *Proc., Conf. Papers in Science*. London: Hindawi.

Li, K., H. Bian, C. Liu, D. Zhang, and Y. Yang. 2015. "Comparison of geothermal with solar and wind power generation systems." *Renewable Sustainable Energy Rev.* 42 (Aug): 1464–1474. https://doi.org/10.1016/j.rser.2014.10.049.

Li, Q., et al. 2020. "Life cycle assessment and life cycle cost analysis of a 40 MW wind farm with consideration of the infrastructure." *Renewable Sustainable Energy Rev.* 138 (2021): 110499.

Ludin, G. A., et al. 2023. "Novel hybrid fault current limiter with hybrid resonant breaker in multi-terminal HVDC transmission system." *Electr. Power Syst. Res.* 221 (Oct): 109403. https://doi.org/10.1016/j.epsr.2023.109403.

Mohammadi, K., A. Mostafaeipour, Y. Dinpashoh, and N. Pouya. 2014. "Electricity generation and energy cost estimation of large-scale wind turbines in Jarandagh, Iran." *J. Energy* 2014 (Nov): 1–8. https://doi.org/10.1155/2014/613681.

Muche, T., R. Pohl, and H. Christin. 2016. "Economically optimal configuration of onshore horizontal axis wind turbines." *Renewable Energy* 90 (May): 469–480. https://doi.org/10.1016/j.renene.2016.01.005.

Noori, A. G., P. A. Salam, and A. M. Fazli. 2019. "Assessment of Selected Biomass Energy Potential in Afghanistan." *Eur. J. Eng. Technol. Res.* 4 (6): 6–14.

Perkin, S., D. Garrett, and P. Jensson. 2015. "Optimal wind turbine selection methodology: A case-study for Búrfell, Iceland." *Renewable Energy* 75 (Feb): 165–172. https://doi.org/10.1016/j.renene.2014.09.043.

Quan, P., and T. Leephakpreeda. 2015. "Assessment of wind energy potential for selecting wind turbines: An application to Thailand." *Sustainability Energy Technol. Assess.* 11 (Aug): 17–26. https://doi.org/10.1016/j.seta.2015.05.002.

Rakhshani, E., H. Mehrjerdi, and A. Iqbal. 2020. "Hybrid wind-diesel-battery system planning considering multiple different wind turbine technologies installation." *J. Cleaner Prod.* 247 (Jan): 119654. https://doi.org/10.1016/j.jclepro.2019.119654.

Rostami, R., S. M. Khoshnava, H. Lamit, D. Streimikiene, and A. Mardani. 2017. "An overview of Afghanistan's trends toward renewable and sustainable energies." *Renewable Sustainable Energy Rev.* 76 (Sep): 1440–1464.

Shah, A., et al. 2023. "Optimization of grid-photovoltaic and battery hybrid system with most technically efficient PV technology after the performance analysis." *Renewable Energy* 207 (May): 714–730. https://doi.org/10.1016/j.renene.2023.03.062.

Siddique, S., and R. Wazir. 2016. "A review of the wind power developments in Pakistan." *Renewable Sustainable Energy Rev.* 57 (Aug): 351–361. https://doi.org/10.1016/j.rser.2015.12.050.

Song, D., et al. 2020. "Optimal design of wind turbines on high-altitude sites based on improved Yin-Yang pair optimization." *Energy* 193 (Aug): 116794. https://doi.org/10.1016/j.energy.2019.116794.

Stehly, T., P. Beiter, and P. Duffy. 2020. *2019 cost of wind energy review.* Rep. No. NREL/TP-5000-78471. Golden, CO: National Renewable Energy Lab.

Sun, H., H. Yang, and X. Gao. 2020. "Investigation into spacing restriction and layout optimization of wind farm with multiple types of wind turbines." *Energy* 168 (2019): 637–650. https://doi.org/10.1016/j.energy.2018.11.073.

Tasneem, Z., et al. 2020. "An analytical review on the evaluation of wind resource and wind turbine for urban application: Prospect and challenges." *Dev. Built Environ.* 4 (Aug): 100033. https://doi.org/10.1016/j.dibe.2020.100033.

Wang, J., X. Huang, Q. Li, and X. Ma. 2018. "Comparison of seven methods for determining the optimal statistical distribution parameters: A case study of wind energy assessment in the large-scale wind farms of China." *Energy* 164 (Aug): 432–448. https://doi.org/10.1016/j.energy.2018.08.201.

Wortman, M. S. 1982. "Strategic management and changing leader-follower roles." *J. Appl. Behav. Sci.* 18 (3): 371–383. https://doi.org/10.1177/002188638201800310.